frontiers | Frontiers in Earth Science

TYPE Original Research
PUBLISHED 15 October 2024
DOI 10.3389/feart.2024.1473101

Check for updates

OPEN ACCESS

EDITED BY
Xiao-Ping Xia,
Chinese Academy of Sciences (CAS), China

REVIEWED BY
Gaoxue Yang,
Chang'an University, China
Fei Wu,
China University of Geosciences
Wuhan, China

*CORRESPONDENCE
Xijun Liu,
xijunliu@glut.edu.cn

RECEIVED 30 July 2024
ACCEPTED 27 September 2024
PUBLISHED 15 October 2024

CITATION
Qu Y, Liu X, Liu X, Huang Q, Yang Q, Hu R, Liu P and Song Y (2024) Petrogenesis and tectonic setting of the proto-tethyan dachaidan ophiolite, North China: insights from clinopyroxene chemistry and whole-rock Sr–Nd–Pb and zircon Hf isotopes.
Front. Earth Sci. 12:1473101.
doi: 10.3389/feart.2024.1473101

COPYRIGHT
© 2024 Qu, Liu, Liu, Huang, Yang, Hu, Liu and Song. This is an open-access article distributed under the terms of the Creative Commons Attribution License (CC BY). The use, distribution or reproduction in other forums is permitted, provided the original author(s) and the copyright owner(s) are credited and that the original publication in this journal is cited, in accordance with accepted academic practice. No use, distribution or reproduction is permitted which does not comply with these terms.

Petrogenesis and tectonic setting of the proto-tethyan dachaidan ophiolite, North China: insights from clinopyroxene chemistry and whole-rock Sr–Nd–Pb and zircon Hf isotopes

Yilin Qu[1,2], Xijun Liu[1,2,3,4]*, Xiao Liu[1,2,3], Qianwen Huang[1,2], Qijun Yang[1], Rongguo Hu[1,2,3], Pengde Liu[4] and Yujia Song[1]

[1]Guangxi Key Laboratory of Hidden Metallic Ore Deposits Exploration, Guilin University of Technology, Guilin, China, [2]Collaborative Innovation Center for Exploration of Hidden Nonferrous Metal Deposits and Development of New Materials in Guangxi, Guilin University of Technology, Guilin, China, [3]Guangxi Science Innovation Base for Formation and Exploration of Strategic Critical Mineral Resources, Guilin University of Technology, Guilin, China, [4]National Key Laboratory of Ecological Security and Resource Utilization in Arid Areas, Xinjiang Institute of Ecology and Geography, Chinese Academy of Sciences, Urumqi, China

Introduction: The Dachaidan ophiolites outcrop within an ultrahigh-pressure metamorphic belt along the northern margin of the Qaidam Basin. However, their age, source, and tectonic setting remain still in debate.

Method: In this study, we investigated the geochemistry and geochronology of the Dachaidan ophiolitic gabbros.

Results and Discussion: Zircon U–Pb dating yielded a crystallization age of 510.0 ± 2.8 Ma and 510.0 ± 2.9 Ma for the gabbro. The gabbros have low SiO_2 contents (47.15–50.10 wt.%) and high MgO contents (6.35–9.04 wt.%) and $Mg^{\#}$ values (55–74). The total rare earth element (∑REE) contents are 8.35–28.07 ppm, lower than those of normal-type mid-ocean ridge basalts (MORBs), and the gabbros exhibit light REE depletion or flat REE patterns, with small positive Eu anomalies (Eu/Eu*= 1.06–1.40). Trace element patterns are depleted to enriched in Nb and Ta, similar to island arc rocks and MORB. Clinopyroxene thermobarometry indicates the parental magma of the gabbros formed by high-temperature (1,318°C–1,363°C) and medium-pressure (1.27–1.64 GPa) partial melting in a mantle wedge. The gabbros have depleted Sr–Nd–Pb-Hf isotopic compositions, with $(^{87}Sr/^{86}Sr)_i$ = 0.704586–0.707441, $\varepsilon_{Nd}(t)$ = 4.7–6.6, and zircon $\varepsilon_{Hf}(t)$ = 7.6–11.4. The age-corrected Pb isotope ratios of these volcanic rocks are variable, with $^{206}Pb/^{204}Pb(t)$ = 18.085–18.253, $^{207}Pb/^{204}Pb(t)$ = 15.595–15.614, and $^{208}Pb/^{204}Pb(t)$ = 37.880–38.148, which are similar to the isotopic compositions of typical Indian MORBs. The source of the Dachaidan ophiolite is inferred to have been depleted mantle. The Dachaidan

ophiolite likely formed in a forearc oceanic setting along the northern margin of the Qaidam Basin, during the initial subduction of an oceanic plate.

KEYWORDS

North Qaidam ultrahigh-pressure metamorphic belt, early paleozoic, gabbro, petrogenesis, tectonic setting

1 Introduction

The Qinling–Qilian–Alxa–Kunlun orogenic belt is the northernmost suture zone of the Proto-Tethys Ocean, and is an ideal region for studying plate convergence, oceanic–continental subduction, magmatism, metamorphism, and deformation (Song et al., 2013). The Qilian orogenic belt extends westward into the Alxa orogenic belt and eastward into the Qinling orogenic belt. The Qilian orogenic belt is a key region for investigating the breakup of Rodinia and accretion of micro-continental blocks along the northern margin of Gondwana. It preserves important information on the tectonic evolution of the Proto-Tethys Ocean. The North Qaidam ultrahigh-pressure (UHP) metamorphic belt (NQUB) is located in the southernmost Qilian orogenic belt, and links the northern Oulongbuluke micro-continental and southern Qaidam blocks. Early Paleozoic deep continental subduction formed HP to UHP metamorphic rocks in this region (Yang et al., 1998; Song and Yang, 2001; Meng et al., 2003; Song et al., 2006; Song et al., 2014a; Song et al., 2004b, Song et al., 2019; Chen et al., 2007; Zhang et al., 2010; Zhang J. X. et al., 2017). Since j1990s, various types of UHP metamorphic rocks, such as eclogite with coesite-bearing quartz (Yang et al., 2001), coesite-bearing garnet peridotite (Zhang et al., 2009a), diamond-bearing garnet pyroxenite (Song et al., 2004b), and K-cymrite-bearing garnet peridotite (Zhang et al., 2009b), have been reported.

About tectonic setting of the NQUB, different researchers shared different opinions. Within the belt, most eclogites show characteristics of intraplate or continental flood basalts, suggesting the NQUB experienced UHP metamorphism (Song et al., 2004a; Xu et al., 2006). Isotopic dating indicates that the protolith ages of most eclogites in the region are 850–750 Ma, with the peak metamorphic ages being 460–420 Ma (Chen et al., 2009; Song et al., 2010; Zhang et al., 2010; Zhang G. B. et al., 2016; Yu et al., 2013). Some eclogites within the belt have geochemical features similar to those of oceanic basalts (Zhang et al., 2008; Zhang et al., 2013), suggestive of oceanic subduction within the NQUB. Zircon dating revealed the protolith of these eclogites formed at 517–514 Ma, with metamorphic ages peak at 457–440 Ma (Zhang et al., 2009a; Zhang et al., 2009b; Zhang et al., 2016), which led to the hypothesis that the NQUB experienced oceanic subduction prior to continental collision and orogenesis. However, controversy persists regarding the timing and tectonic evolution of oceanic subduction and processes in the NQUB. Yin et al. (2007) suggested that the NQUB resulted from southward subduction of the North Qilian oceanic crust, subduction of trench sediments, and uplift of overlying continental crustal materials. Zhang et al. (2013) proposed that northward oceanic subduction occurred from 540 to 450 Ma, followed by a period of continental subduction from 450 to 420 Ma. Song et al. (2014a) proposed a relationship between the NQUB and North Qilian orogenic belt, suggesting that the NQUB formed due to northward oceanic subduction in the North Qilian Ocean, which resulted in deep continental subduction of the Qilian–NQUB block. In this model, the period from 460 to 440 Ma is considered to have been characterized by oceanic subduction, whereas deep continental subduction occurred from 440 to 420 Ma.

Most of research the NQUB focused on the Yuka, Lvliangshan, Xitieshan, and Dulan areas, including the geological and geochemical characteristics of eclogites, garnet-bearing (ultra) mafic rocks, and intermediate–silicic intrusive rocks. For examples, previous studies have investigated eclogites, orthopyroxene-bearing garnet peridotites, and pyroxenitic garnet lherzolites in the Shaliuhe (Dulan) and Chachahe areas (Hao et al., 2001; Wang et al., 2020; Ren et al., 2022; Wang et al., 2022). In the Lvliangshan region, there are two types of eclogite: blocky and banded. The banded eclogites are considered to be metamorphosed crustal rocks of the Dakendaban Formation (Wang et al., 2001), which record two orogenic cycles. The Yuka–Luofengpo eclogites were associated with the early orogenic cycle related to the assembly and breakup of the Rodinia supercontinent during the Paleo-Proterozoic, and a later orogenic cycle in the Early Paleozoic associated with oceanic expansion, subduction, and continent–continent collision (Ren et al., 2019). Wu et al. (2008) investigated granites in the Sanchagou area in the western NQUB and suggested that, during the middle Permian, the NQUB was in a post-collisional intracontinental subduction setting. Dong et al. (2014) suggested that the late Permian granites along the northwestern margin of the Oulongbuluke Block formed in a volcanic arc, indicating the NQUB was experiencing oceanic–continental subduction during the late Permian. However, Gao et al. (2019) proposed that the NQUB was already underwent oceanic–continental subduction in the middle Permian. Further research is needed to resolve these issues.

Due to the close relationship between the geochemical characteristics of (ultra) mafic igneous rocks and their tectonic setting and mantle source, such rocks that formed during different tectonic stages have distinct geochemical features. These rocks can constrain crust-mantle interactions, deep mantle properties, and the tectonic evolution of orogenic belts (Li et al., 1995; Zhang et al., 1995; Cheng et al., 2016). Therefore, determining the evolution of the NQUB requires a systematic investigation of its (ultra) mafic rocks, particularly the ophiolite. This involves determining their ages, tectonic setting, and petrogenesis.

This study focused on the gabbros in the Dachaidan ophiolite in the NQUB. Based on detailed field investigations, systematic sampling was conducted, and the samples were subjected to petrological, zircon U–Pb geochronological, mineral and whole-rock geochemical, and Sr–Nd–Pb–Hf isotope analyses, in order to constrain their source characteristics and petrogenesis. Combining the results and regional geological data to provide new constraints

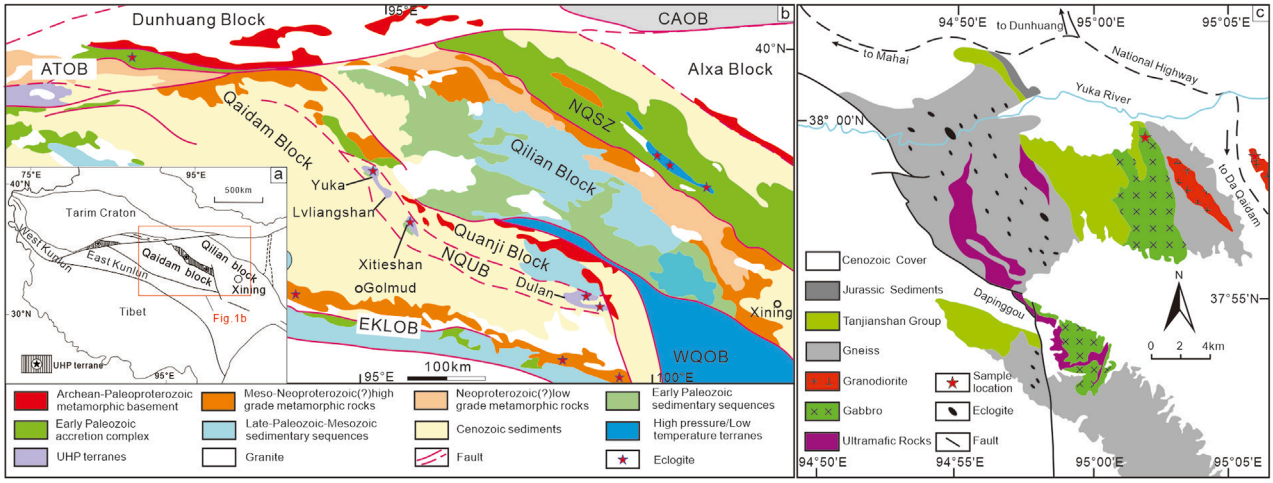

FIGURE 1
(A) Sketch tectonic map showing the location of the Qaidam Block on the Tibetan Plateau. **(B)** Geological map of North Qaidam (modified after Zhang J. X. et al., 2017) and **(C)** geological map of the Lvliangshan area (modified after Ren et al., 2019). CAOB, Central Asian Orogenic Belt; NQSZ, North Qilian suture zone; NQOB, North Qaidam orogenic belt; WQOB, West Qinling orogenic belt; ATOB, Altyn orogenic belt; EKLOB, East Kunlun orogenic belt.

on the tectonic setting and evolution of the NQUB and subduction in the northern Proto-Tethys.

2 Geological background and sample descriptions

2.1 Geological background

The NQUB is located on the northeastern margin of the Qinghai–Tibetan Plateau within Qinghai Province, China. It extends along the northern margin of the Qaidam Basin in a WNW–ESE orientation. To the north, it is bordered by the Qilian terrane, while the Qaidam terrane lies to the south. To the east, it connects with the Qinling orogenic belt (Figure 1). To the westernmost of NQUB, it cut by the Altun strike-slip fault. Approximately 300 km north of this belt is the Northern Qilian suture zone, which formed during the Caledonian Orogeny and is characterized by ophiolitic and low-temperature–high-pressure metamorphic rocks (Zhang et al., 2012). From west to east, the NQUB contains the Lvliangshan–Yuka, Xitieshan, and Dulan UHP metamorphic units. The rocks exposed within this belt were derived primarily from sedimentary protoliths and include paragneiss and granitic gneiss. In addition, eclogite, mafic granulite, and lens-shaped occurrences of garnet-bearing olivine gabbro occur in this region (Song et al., 2013).

The Oulongbuluke micro-continent is located between the Qilian terrane and the NQUB. This micro-continent has Neoproterozoic to Paleoproterozoic crystalline basement, with geological affinities to the South China Block. It has been proposed that the Oulongbuluke micro-continent separated from the South China Block at *ca.* 780 Ma, during subduction in the NQUB and leading to the migration of the micro-continent to the southern margin of the Qilian terrane. During the Early Paleozoic, a continental arc developed on the fragmented continental basement, transforming the Oulongbuluke micro-continent into an active continental margin (Xiao et al., 2009; Tung et al., 2012; Tung et al., 2013; Yan et al., 2015). Following closure of the North Qaidam Ocean, the Qaidam Block collided with the southern Oulongbuluke micro-continent within the southern Qilian terrane. This collisional event ultimately led to the formation of the NQUB.

The Tanjianshan Group consists of lower Paleozoic strata that are widespread in the NQUB, which crop out in a NW–SE orientation. The group is in fault contact with the Archean Dawan Group and is in contact with strata of different ages via either faults or angular unconformities. The lower part of the Tanjianshan Group consists of intermediate–mafic submarine volcanic rocks, while the upper part consists of clastic and carbonate rocks. Based on fossil assemblages, isotopic dating, and tectonothermal events, Gao et al. (2011) suggested that the Tanjianshan Group formed in an island arc and represents the products of different stages of oceanic–continental subduction during the early Paleozoic (510–460 Ma; i.e., Cambrian–Ordovician).

Our study area is located in the Dachaidan region to the west of the NQUB. The main faults within the belt are NW–SE-trending. In this region, the ophiolite unit is well-exposed and the different rock types are in tectonic contact. The lower stratigraphic units are strongly serpentinized and metamorphosed peridotites, while the middle units are metamorphosed cumulate gabbros (pyroxenites), with locally developed igneous cumulate textures. These textures are characterized by alternating light-colored bands with relatively high-An plagioclase and dark-colored bands with relatively high contents of mafic minerals. The upper units consist of volcanic rocks (i.e., amphibolites) of the Tanjianshan Group, which are intercalated with abundant pyroxenite (Zhu et al., 2014). In addition, this region contains outcrops of Precambrian metamorphosed basement (i.e., the Archean Dawan Group). The protoliths of these rocks include volcanic and clastic rocks, which have underwent medium-to high-grade metamorphism.

Geochronological studies indicate that the age of the granitic gneiss in this region is *ca*. 952 Ma, which is production of crustal melting (Lin et al., 2006). There are outcrop two types of eclogite: (1) lens-shaped bodies within the granitic gneiss and (2) in association with the metamorphosed crustal rocks, which have either lens-shaped or layered structures. Ren et al. (2019) discovered eclogites with mid-ocean ridge basalt (MORB) characteristics in the Yuka–Luofengpo area, which have ages of 1,280–1,070 Ma. These eclogites are considered to be remnants of the Mesoproterozoic Mirovoi Ocean surrounding Rodinia superterrane, which underwent two utral high-pressure metamorphism during the Neoproterozoic (amphibolite facies) and Early Paleozoic (UHP metamorphism).

2.2 Sample descriptions

The gabbros have underwent variable degrees of metamorphism and have been transformed into amphibolite with a gray–green color, granular crystalline texture, and blocky fabric (Figures 2A, B). The main minerals include pyroxene (40 vol.%), clinopyroxene (30 vol.%), and hornblende (30 vol.%) (Figures 2C–F).

3 Analytical methods

All analyses were carried out at the Guangxi Key Laboratory of Hidden Metallic Ore Deposits Exploration, Guilin University of Technology, Guangxi, China. Zircon U-Pb dating and mineral trace element analyses were conducted with a 193 nm COMPexPro 102 ArF excimer LA system (GeoLas HD, Gottingen, Germany) coupled to an Agilent 7,900 quadrupole ICP-MS (i.e., LA–ICP–MS). Whole-rock major and trace elements were analyzed with a ZSX Primus II X-ray fluorescence (XRF) spectrometer and an Agilent 7500cx ICP-MS, respectively. The major element contents of minerals were measured with a JEOL JXA–8230 electron probe microanalyzer (EPMA). Zircon Hf isotope analyses of the same zircon grains were conducted with an ArF excimer LA system attached to a Neptune Plasma MC-ICP-MS. Whole–rock Sr–Nd–Hf isotope ratios were measured in solution with a Neptune plus multicollector (MC)–ICP–MS. The analytical methods are described in detail in the Supplementary Text.

4 Results

4.1 Zircon U–Pb geochronology

Zircon U–Pb isotopic dating was conducted on gabbro sample DC-399 and DC-400 from the Dachaidan ophiolite. Forty zircon grains were selected for analysis, and their CL images are predominantly gray–black, with some appearing white. The zircon shape with elongate or short prismatic, and irregular shapes (Figure 3A), with length:width ratios of 1:1 to 2:1. Individual zircon U–Pb ages for each grain are presented in Supplementary Table S1. The U and Th contents of the 40 zircon grains, they are 165–2037 and 143–3,225 ppm, respectively. The Th/U ratios range from 0.57 to 2.19, which are typical of magmatic zircons (Hoskin and Black, 2000). The $^{206}Pb/^{238}U$ ages of the 40 zircon grains in the gabbro exhibit minimal variation and vary from 502 to 520 Ma. The weighted-mean ages are 510.0 ± 2.8 Ma and 510.0 ± 2.9 Ma, which represents the crystallization age of the gabbro. This indicates that the ophiolite in this region formed during the middle Cambrian. On a chondrite-normalized rare earth element (REE) diagram, the zircon grains exhibit light REE depletion, heavy REE enrichment ($[Gd/Yb]_N$ = 0.029–0.103), and distinct positive Ce and negative Eu anomalies (Figures 3C, E).

4.2 Whole-rock major and trace elements

Apart from sample DC-399, which has a LOI value of 5.01 wt.%, most of the gabbro samples from the Dachaidan ophiolite have low LOI values (<3 wt.%), indicative of minimal weathering. The gabbros have relatively low and uniform SiO_2 (47.15–49.63 wt.%) and TiO_2 (0.26–0.75 wt.%) contents. The samples have elevated contents of Al_2O_3 (14.84–16.25 wt.%) and MgO (6.35–9.04 wt.%), resulting in $Mg^{\#}$ ($Mg^{\#}$ = molar MgO/[MgO + $Fe_2O_3{}^T$] × 100) values of 55–74. These elevated MgO contents and $Mg^{\#}$ values are indicative of a mafic parental magma. The total alkali contents (K_2O + Na_2O) of the gabbros range from 2.52 to 3.00 wt.% (Supplementary Table S2). On the Zr/TiO_2–Nb/Y diagram used for classifying igneous rocks (Figure 4), the samples plot into the gabbro field.

In a chondrite-normalized trace element diagram (Figure 5A), the gabbros are characterized by depletions of light REEs to flat REE patterns $(La/Yb)_N$ ratios are 0.51–1.06, indicative of moderate enrichment in light REE. In addition, there are obvious positive Eu anomalies, with Eu/ ∗ Eu values ($2Eu_N/[Sm_N + Gd_N]$) of 1.06–1.40. The gabbros have relatively low and uniform total REE contents (ΣREE = 8.35–28.1 ppm; average = 15.82 ppm). This average is less than that of normal-type MORBs (N-MORBs; ΣREE = 39.1 ppm; Sun and McDonough, 1989). On a primitive-mantle-normalized trace element diagram (Figure 5B), the gabbros exhibit depletions in Th and U, and positive Sr anomalies. These trace element features, and the positive Eu anomalies and lower ΣREE contents than N-MORBs, can be attributed to plagioclase accumulation in the gabbros. The results are listed in Supplementary Table S2.

4.3 Whole-rock Sr–Nd-Pb and zircon Hf isotopes

Whole-rock measured and initial Sr–Nd isotope ratios for the gabbros in the Dachaidan area are listed in Supplementary Table S3 and shown in Figure 6. The gabbros exhibit significant variations in $(^{87}Sr/^{86}Sr)_i$ from 0.704586 to 0.707441, which are much higher than depleted mantle source, may have been affected by alteration. The initial Nd isotope ratios are also indicative of a depleted mantle source, with $\varepsilon_{Nd}(t)$ = +4.68 to +6.59 (Supplementary Table S3). The initial Sr–Nd isotopic compositions of the gabbros are similar to those reported for basalts from the Lajishan oceanic plateau ($(^{87}Sr/^{86}Sr)_i$ values (0.70434–0.70704), $\varepsilon_{Nd}(t)$ values (0.9–8.9)), as well as the Yuka boninites ($(^{87}Sr/^{86}Sr)_i$ values (0.7054~0.7065), and the ε_{Nd} (t) values (4.1~6.1)) and magnesian andesites ($(^{87}Sr/^{86}Sr)_i$

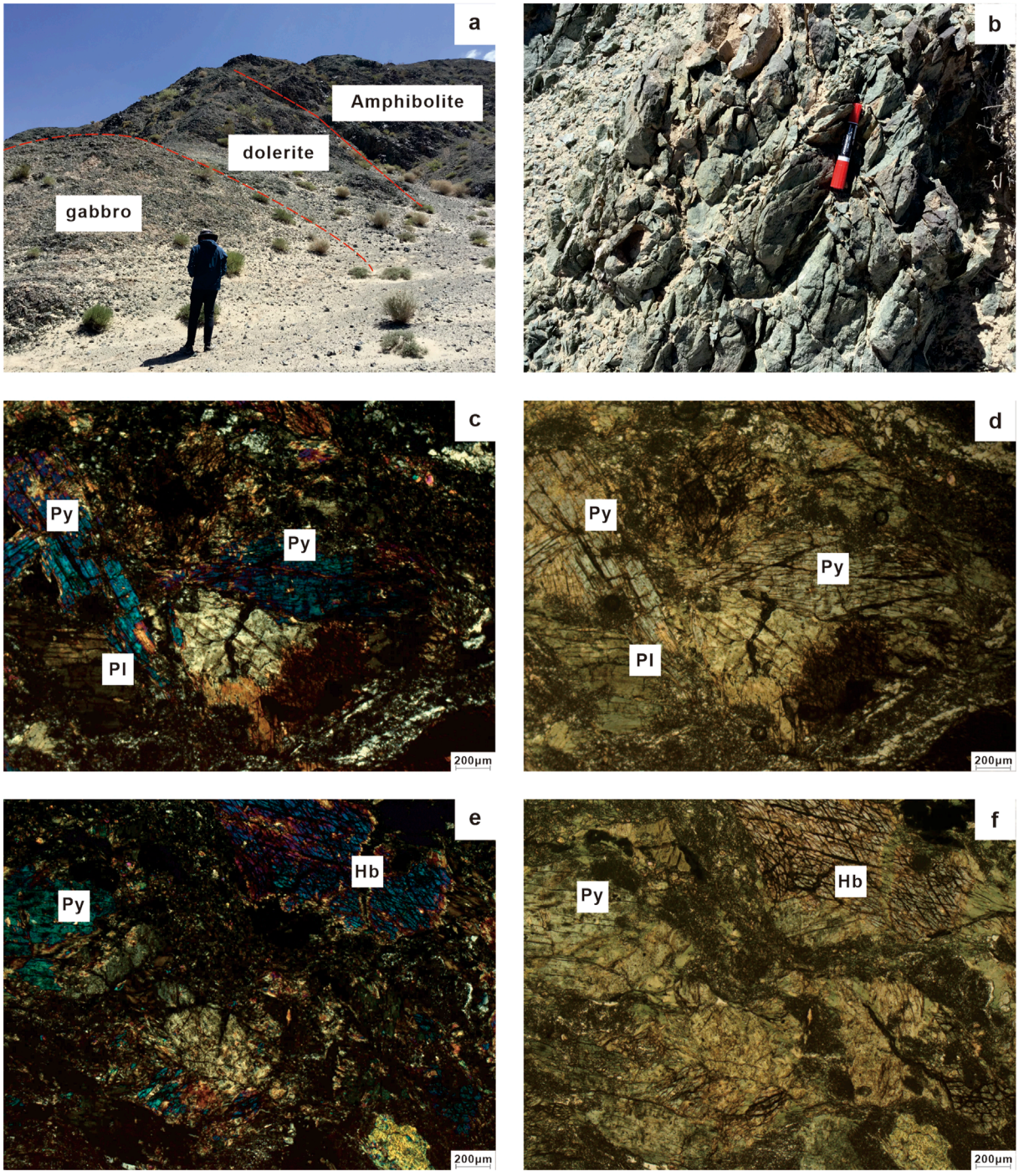

FIGURE 2
(A, B) Field photographs, and **(C, E)** plane- and **(D, F)** cross-polarized light photomicrographs of the Dachaidan gabbros. Mineral abbreviations: Hb, hornblende; Pl, plagioclase; Py, pyroxene.

values (0.7059~0.7067)), and ε_{Nd} (t) values (2.5~5.3), and Proto-Tethyan oceanic ophiolites in the region (Figure 6A). The age-corrected Pb isotope ratios of these volcanic rocks are variable, with $^{206}Pb/^{204}Pb(t)$ = 18.085–18.253, $^{207}Pb/^{204}Pb(t)$ = 15.595–15.614, and $^{208}Pb/^{204}Pb(t)$ = 37.880–38.148. In plots of ^{207}, $^{208}Pb/^{204}Pb$ vs $^{206}Pb/^{204}Pb$ (Figures 6C, D), all the samples plot above the Northern Hemisphere Reference Line (NHRL) and are similar to the isotopic compositions of typical Indian MORBs.

The zircon Lu–Hf isotope data for gabbro sample DC-399 and DC-400 are listed in Supplementary Table S4. The initial Hf isotope ratios of the Dachaidan gabbros vary from 0.282678 to 0.282837. The weighted-mean is 0.282751, with a corresponding $\varepsilon_{Hf}(t)$ value of

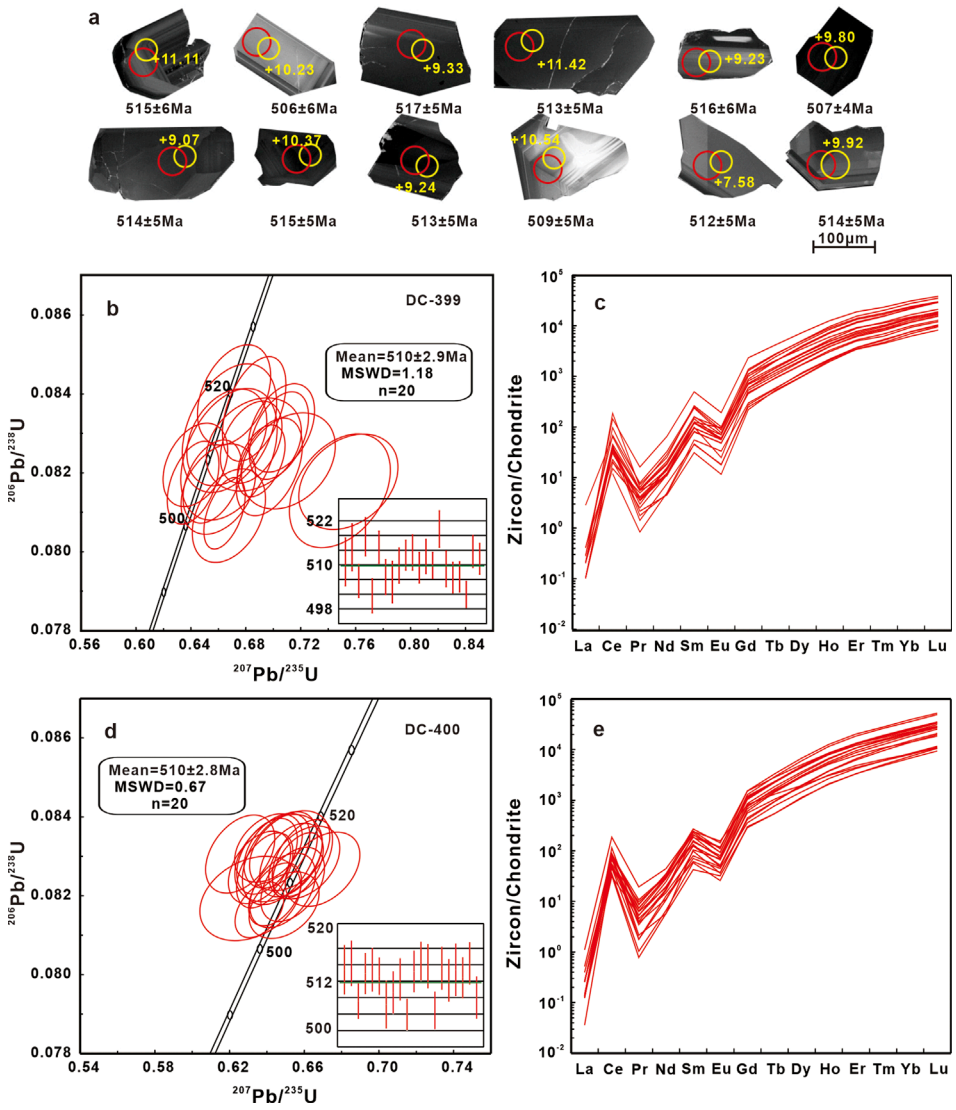

FIGURE 3
(A) Partial Zircon CL images, **(B,D)** U–Pb concordia diagram, and **(C,E)** chondrite-normalized REE patterns for the Dachaidan gabbros. The red circles represent the sites of zircon U–Pb dating analyses and the yellow circles represent the locations of zircon Hf isotope analyses.

+10.0. All data plot above the chondritic uniform reservoir evolution line, indicative of a depleted mantle source (Figure 6B). Single-stage Hf isotope model ages (t_{DM1}) vary from 812 to 661 Ma, while two-stage Hf isotope model ages (t_{DM2}) range from 977 to 731 Ma.

4.4 Clinopyroxene chemistry

We analyzed a relatively fresh clinopyroxene phenocryst (in sample DC-400) from a Dachaidan gabbro. Cation contents were calculated based on six oxygen atoms (Supplementary Table S5). In back-scattered electron images of clinopyroxene within the gabbro, most clinopyroxene grains do not exhibit compositional zoning. They occur as large phenocrysts (2–10 mm, but typically 3–6 mm), microphenocrysts (0.5–1.0 mm), and microcrysts within the matrix (Figures 5–8). The SiO_2 contents are 48.31–51.20 wt.%, MgO contents are 13.21–15.00 wt.%, $Mg^{\#}$ values are 63–70, CaO contents are 11.60–12.32 wt.%, FeO contents are 13.38–16.45 wt.%, and TiO_2 contents are 0.10–0.42 wt.%. Based on the Wo–En–Fs ternary diagram, the pyroxene can be classified as augite.

Chondrite-normalized REE patterns and a primitive-mantle-normalized trace element diagram for the clinopyroxenes are shown in Figures 8A, B. All the clinopyroxenes have similar REE and trace element patterns, suggestive of a common origin. The ΣREE contents are relatively low (13.50–173.88 ppm), with $(La/Sm)_N$ = 0.21–0.92 and $(La/Yb)_N$ = 0.19–1.29 (Supplementary Table S5). These values are indicative of significant depletion of light REEs as compared with middle and heavy REEs (Figure 8A), and are associated with

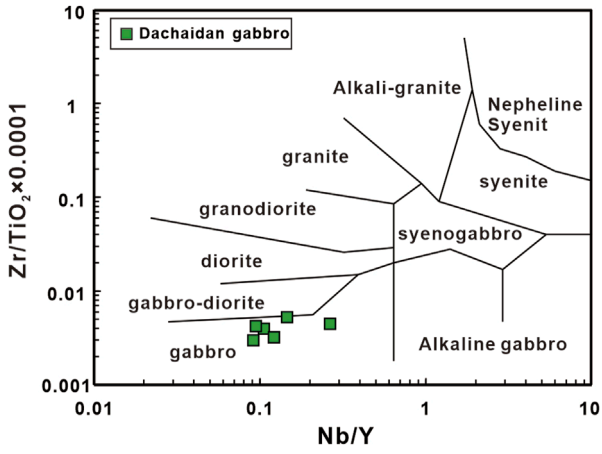

FIGURE 4
Zr/TiO_2–Nb/Y diagram for the Dachaidan gabbros (after Winchester and Floyd, 1977).

significant negative Eu anomalies (Eu/Eu^* = 0.15–0.77). Compared with gabbro sample DC-400, the clinopyroxenes exhibit clear depletions in Sr, Eu, Nb, Ta, Zr, and other REEs (Figure 8B).

5 Discussion

5.1 Effects of alteration

Microscopic observations indicate that metamorphic processes have affected the Dachaidan gabbros, resulting in well-developed amphibolite-facies mineral assemblages, particularly the presence of hornblende (Figures 2C, D). Although alteration and metamorphic processes often mobilize large-ion lithophile elements (e.g., K, Rb, Sr, Ba, Cs, and Pb), REEs and high-field-strength elements (e.g., Nb, Ta, Zr, Hf, Th, and Ti) tend to remain relatively immobile (Hajash, 1984; Zhu et al., 2008; Escuder et al., 2010). This study predominantly relies on these less-mobile elements for the following discussion.

The gabbros have relatively high initial Sr isotope ratios of 0.704586–0.707434, with an average of 0.705737 (Supplementary Table S3). This is broadly equivalent to the Sr isotope ratios of MORBs (0.70229–0.70613; Saunders et al., 1988), but higher than the Sr isotope ratios of ocean island basalts (OIBs), as typified by Hawaiian volcanic rocks with $^{87}Sr/^{86}Sr$ = 0.70317–0.70412 (Stille et al., 1983). The elevated initial Sr isotope ratios may be due to contamination by crustal materials or subsequent seawater alteration. The gabbros in this region have only experienced minor crustal contamination, indicating seawater alteration is the likely cause of the elevated initial Sr isotope ratios.

Ophiolites are remnants of oceanic lithosphere and commonly underwent metasomatism by mantle fluids and subsequent seawater alteration during their formation. Strontium is a relatively mobile element and is susceptible to various post-magmatic alteration processes. In a $\varepsilon_{Nd}(t)$–$^{87}Sr/^{86}Sr$ diagram, $\varepsilon_{Nd}(t)$ is almost constant with increasing $^{87}Sr/^{86}Sr$ (Figure 6A), which can be interpreted as the result of fluid metasomatism or seawater alteration (McCulloch et al., 1980). Neodymium is immobile element, and the Nd isotope ratio of weakly altered seafloor rocks remains largely unchanged until the water/rock ratio reaches 10^5 (McCulloch et al., 1981). In addition, zircon is a stable mineral that is hard to altered during weathering and metasomatic reaction, and consequently preserves its elemental and isotopic composition while its formation (Li et al., 2009).

5.2 Composition of the mantle source

The La/Yb ratio can be an indicator of the depth of source melting. A lower La/Yb ratio suggests shallow melting, with spinel being the primary residual phase in the source. Conversely, a higher La/Yb ratio indicates deeper melting, with garnet being the main residual phase in the source (Yang et al., 2007). The relatively low La/Sm, Sm/Yb, and Dy/Yb ratios of the studied samples suggest that partial melting occurred in a spinel lherzolite source and similar to the IBM forearc ophiolite mantle source (Figure 9; Zhang et al., 2008).

Lead is a fluid-mobile element and is added to the mantle in the form of slab-derived fluids or sediment melts, which modifies the Pb isotopes in the mantle (Pearce and Peate, 1995). The addition of a small number of subducted sediments will change the Pb isotopic composition from that of depleted mantle to that of the subducted sediments (Kersting and Arculus, 1994). Therefore, Pb isotope data is a sensitive indicator for the involvement of subduction components in the mantle source. As such, we undertook three-component mixing in Nd–Pb isotope space (Figures 6E, F) to further constrain the nature of the subduction components. The modeling results suggest that less than 10% of a subduction component with variable amounts of slab-derived fluid and sediment melt could have generated the source of the parental melts of the Dachaidan gabbros. Previous studies have found that ophiolite altered by ocean floor alteration exhibits significant positive Eu anomalies (Philpotts et al., 1969; Sun and Nesbitt, 1978), therefore, we believe that the mantle source of Dachaidan gabbros has been mixed with slab-derived fluid, leading to Eu positive anomalies.

$\varepsilon_{Nd}(t)$ values for the Dachaidan gabbros range from +4.7 to +6.6, indicative of derivation from a depleted mantle source. In general, if zircon $\varepsilon_{Hf}(t) > 0$, the source is depleted mantle or newly formed young crust derived from depleted mantle. For the Dachaidan gabbros, the zircon $\varepsilon_{Hf}(t)$ values of +7.6 to +11.4 indicate an isotopically depleted mantle source.

5.3 Crystal fractionation

The Dachaidan gabbros have moderate MgO contents (6.35–9.04 wt.%) and $Mg^{\#}$ values (55–74), with low contents of Cr (22–272 ppm) and Ni (65–94 ppm), and do not contain olivine. This suggests olivine fractionation occurred during magma evolution. As $Mg^{\#}$ decreases, Cr and Ni contents, and CaO/Al_2O_3 ratios also decrease, indicative of fractionation involving olivine and clinopyroxene (Figures 10A–D). $Mg^{\#}$ values are used as an indicator of fractional crystallization, with $Mg^{\#}$ >60 indicative of a (near-) primary magma (Langmuir et al., 1977). Samples DC-400, -401, and –402 have relatively high $Mg^{\#}$ values of 65–74, similar to primary

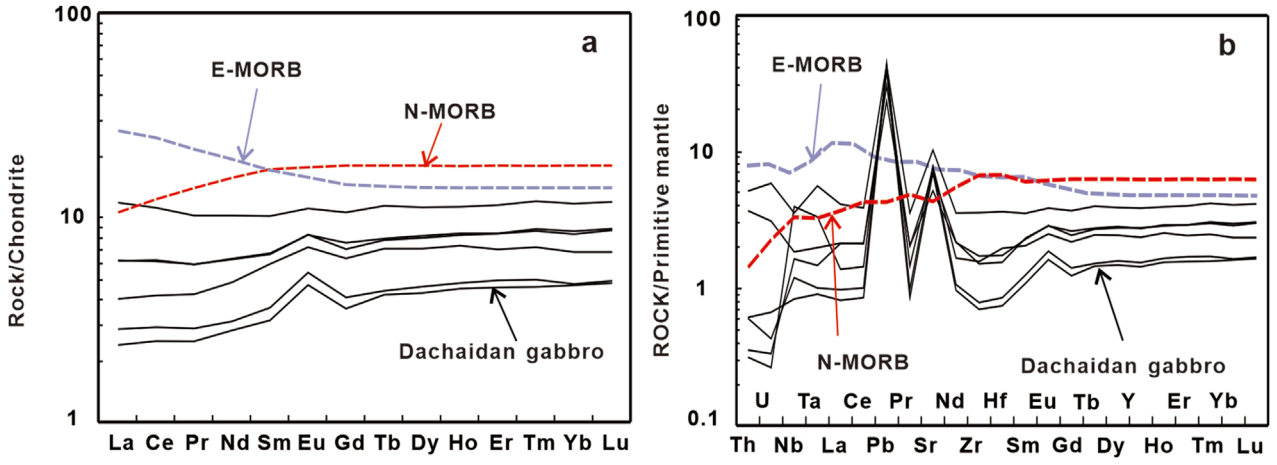

FIGURE 5
(A) Chondrite-normalized REE patterns and **(B)** primitive-mantle-normalized multi-element diagram for the Dachaidan gabbros (after Sun and McDonough, 1989).

magmas. Conversely, samples DC-396 and -399 have $Mg^{\#}$ = 55–59, indicative of fractional crystallization.

The composition of clinopyroxene can provide important information on the magma evolution, including the type of parental magma, and the temperature and pressure of crystallization (Leterrier et al., 1982). Igneous thermobarometers can provide important insights into magma formation, and thus these were applied to the Dachaidan gabbros (Putirka, 2008).

The clinopyroxene in the gabbro is euhedral–subhedral and has relatively uniform major and trace element compositions. This suggests the clinopyroxenes crystallized in a relatively closed magmatic system (Carracedo, 1999). By calculating the equilibrium constant K_D $(Fe–Mg)^{cpx/liq}$, the state of equilibrium between clinopyroxene and the host rock can be determined. Based on experimental results, when K_D $(Fe–Mg)^{cpx/liq}$ is 0.2–0.4 the clinopyroxene and host magma are in equilibrium (Liotard et al., 1988). We used the formula of Wood (1997) (K_D $[Fe–Mg]^{cpx/liq}$ = 0.109 + 0.186 × $Mg^{\#}_{cpx}$) to calculate the equilibrium constant for the studied clinopyroxene. The range of K_D $(Fe–Mg)^{cpx/liq}$ values for the clinopyroxenes is 0.226–0.239, indicative of equilibrium between clinopyroxene and the host magma. Therefore, the temperature and pressure calculated from clinopyroxenes in the Dachaidan gabbros can constrain the physicochemical conditions during magma formation.

We used the clinopyroxene–melt equilibrium thermobarometer of Putirka (2008) to calculate the temperatures and pressures (Supplementary Table S5). The crystallization temperatures range from 1,326°C to 1,363°C, with an average of 1,341°C. The crystallization pressures vary from 1.27 to 1.64 GPa, with an average of 1.47 GPa.

To gain further insights into the gabbroic magmas, a comparison was made with MORB samples from the Mid-Atlantic Ridge and East Pacific Rise. The *P–T* data calculated using the clinopyroxene thermobarometer plot within the anhydrous melting field for mid-ocean ridges (Figure 11), indicating the Dachaidan gabbros formed in a high-temperature, moderate-pressure, anhydrous melting environment. The *P–T* conditions of melting for the Dachaidan gabbros are similar to those of MORBs.

In summary, the primary magmas of the Dachaidan gabbros were derived from depleted mantle, and partial melting occurred in spinel-facies mantle. There was then some fractional crystallization of minerals such as olivine and clinopyroxene, which ultimately resulted in the formation of the Mg-rich gabbros.

5.4 Tectonic setting

In the context of ophiolite formation, some studies have proposed that only a small proportion of ophiolites are the product of mid-ocean ridge spreading, and most form in supra-subduction zones (Pearce et al., 1984). Gabbros in ophiolites are derived from the mantle by partial melting and/or underwent subsequent fractional crystallization. Therefore, gabbros in ophiolites can constrain the geochemical characteristics of ophiolites in orogenic belts and provide insights into the tectonic setting of ophiolite formation.

Island arc basalts (IABs) and depleted MORBs typically have Ta and Nb contents of <0.7 and <12 ppm, respectively, with Nb/La <1, Hf/Ta >5, La/Ta >15, and Ti/Y <350. In contrast, within-plate basalts (WPBs), transitional MORBs (T-MORBs), and enriched MORBs (E-MORBs) have opposite features (Condie, 1989). The Dachaidan gabbros have low Ta (0.04–0.23 ppm) and Nb (0.59–2.79 ppm) contents, with Nb/La = 0.80–2.97, Hf/Ta = 4.91–7.95, La/Ta = 7–24, and Ti/Y = 195–260. Although some samples have low La/Ta ratios, the elemental abundances and ratios of the Dachaidan gabbros are similar to those IABs or depleted MORBs. In Figure 12, the Dachaidan gabbros plot near the N-MORB trend and similar to the IBM forearc basalts mantle source.

In the 2Nb–Zr/4–Y tectonic discrimination diagram (Figure 13A), the samples plot near the N-MORB and volcanic arc basalt fields, similar to Yuka MORB-like gabbros and basalts, and Lashuixia gabbros. In the V–Ti/1,000 diagram (Figure 13B),

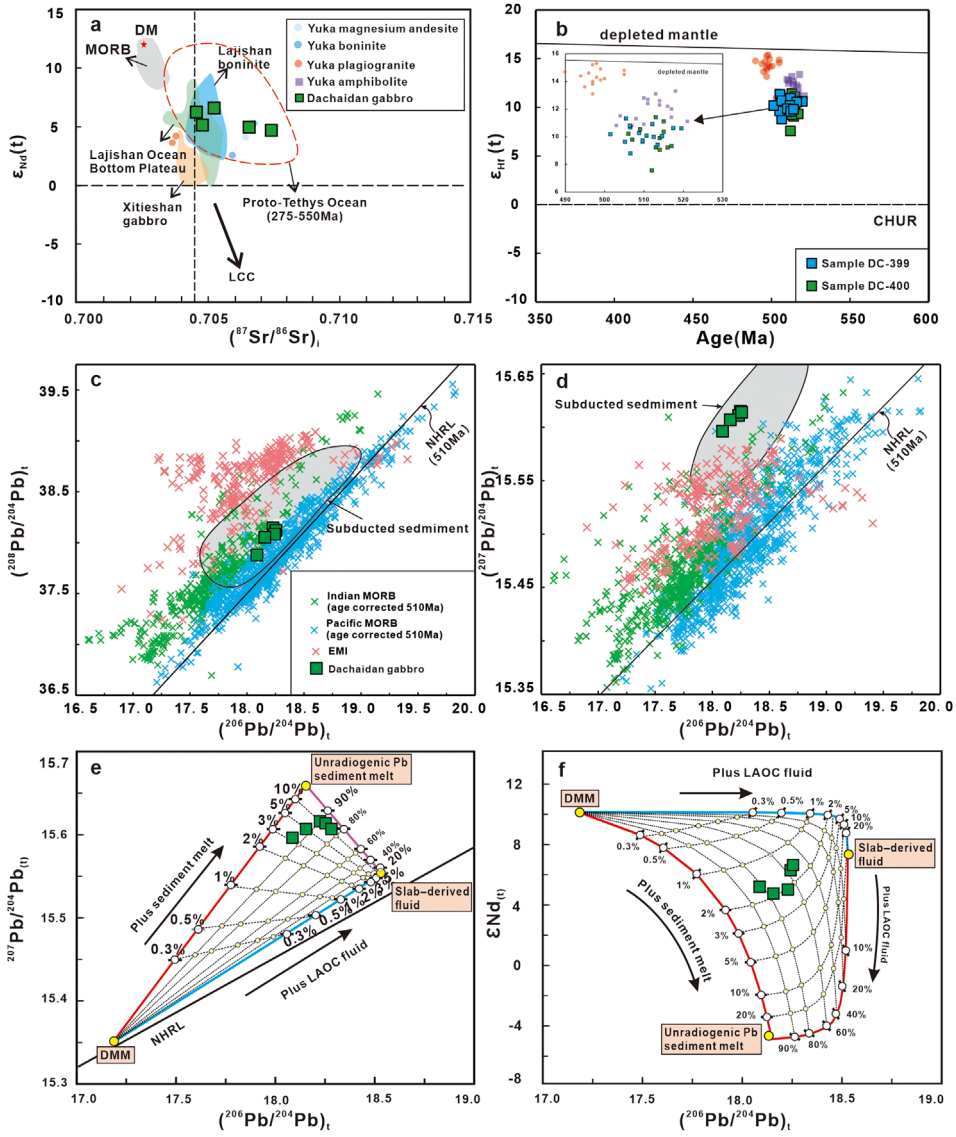

FIGURE 6
Sr-Nd **(A)**, zircon Hf **(B)** and Pb **(C,D)** isotope plots for the Dachaidan gabbros (Proto-Tethys data are from Liu et al., 2021; basalt data for the Lajishan oceanic plateau are from Zhang et al., 2017; Lajishan boninite data are from Yang et al., 2019; Xitieshan gabbro data are from Sun, 2020, Pacific, North Atlantic, Indian MORB and data are from the Pet DB database (http://www.petdb.org/) and the compilation of Stracke et al., 2003; the Northern Hemisphere Reference Line (NHRL) is from Hart, 1984). And three-component mixing model on plots of $^{206}Pb/^{204}Pb(t)$ vs. $^{207}Pb/^{204}Pb(t)$ **(E)** and $_{\varepsilon Nd}(t)$ vs $^{206}Pb/^{204}Pb(t)$ **(F)** for the Dachaidan gabbros (after Zhang et al., 2021), showing the amounts of Nd, Hf, and Pb from the subduction component that affected the source of the Dachaidan gabbros.

the samples plot in the IAB field, indicative of a subduction-related origin. In summary, the Dachaidan ophiolite exhibits the geochemical features of both N-MORBs and IABs. Volcanic rocks with such characteristics are typically associated with forearc basins above subduction zones (Xu et al., 2003; Tian et al., 2008; Reagan et al., 2010). Forearc basin volcanic rocks typically include basalts and high-Mg andesites. Previous studies in the Yuka–Kaipinggou area have identified basalt, IAB, and magnesian andesite (Zhu, 2011; Zhu, 2021; Tuo, 2019), similar to the IBM forearc basalts (Ishizuka et al., 2014). Implying a possible forearc tectonic origin for the Dachaidan gabbro. In the V–Ti/1,000 diagram (Figure 13B), all samples plot within the Izu–Bonin–Mariana Forearc basalts and boninite fields. In addition to the above evidence, the TiO_2, MgO, and FeO^T contents of the samples in this study are similar to those of IBM basalt (TiO_2 from 0.67 to 1.64, MgO from 4.62 to 9.76 and FeO^T content of 8.88–14.16) (Figures 13C, D).

Due to the resistance of clinopyroxene to alteration during low-grade metamorphism and late-stage magmatic processes, its composition is useful for determining the tectonic setting (Leterrier et al., 1982). The SiO_2, TiO_2, and Al_2O_3 contents of clinopyroxene are controlled mainly by its composition rather than the physicochemical conditions of crystallization (Brown et al.,

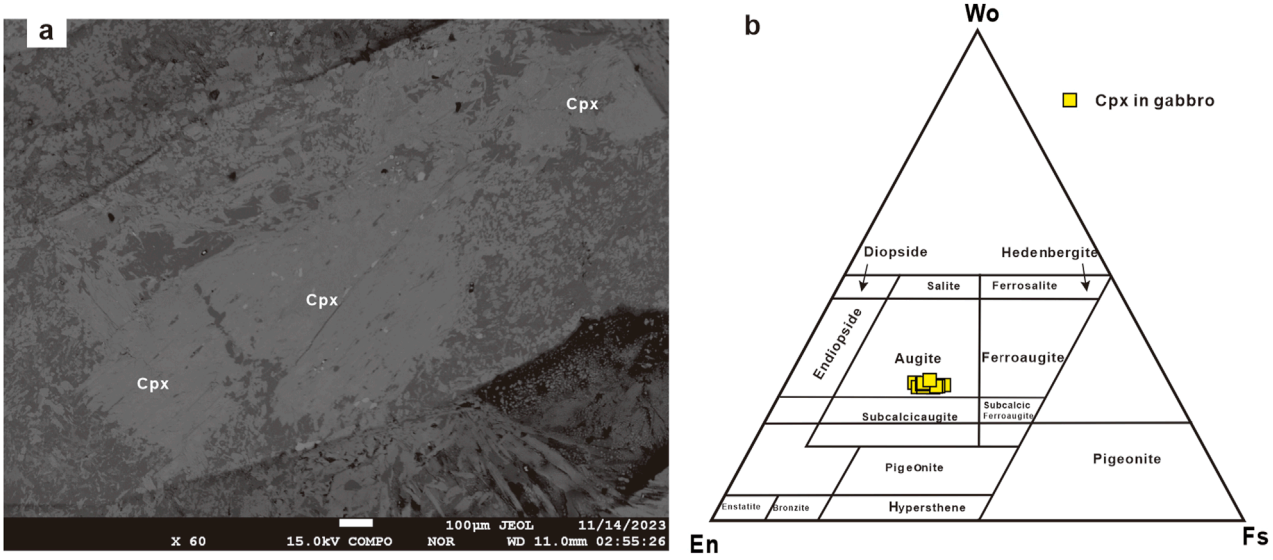

FIGURE 7
(A) Back-scattered electron image of sample DC-400. (Cpx = pyroxene) and **(B)** ternary classification diagram of the analyzed pyroxenes.

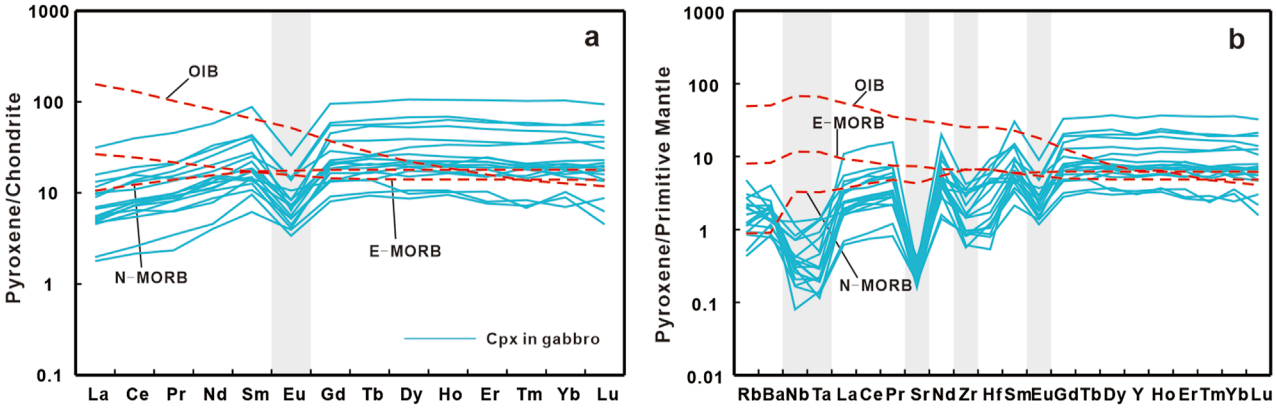

FIGURE 8
(A) Chondrite-normalized REE patterns and **(B)** primitive-mantle-normalized trace element diagram for clinopyroxenes in the Dachaidan gabbros.

1967). In the TiO_2–SiO_2/100–Na_2O ternary diagram, the Dachaidan gabbros plot in the field for island arc tholeiites (IATs) and forearc basaltic andesites (BA-A). In a Ti–Al (atomic proportions) diagram (Figure 14B), most clinopyroxene plots in the fields for IATs, BA-A, and basaltic andesite (BA). The clinopyroxene in the Dachaidan gabbros has lower Ti contents and Ti/V ratios than MORB and BABB, similar to IATs and low-Ti basaltic andesites (Figure 14C), indicative of crystallization from a high-Mg magma. This is consistent with the high $Mg^{\#}$ values of the gabbro samples. Melting of a mantle wedge during subduction of hot and young oceanic lithosphere likely led to ophiolite formation under high-temperature and medium-pressure conditions. Both the whole-rock and clinopyroxene geochemical data confirm that the Dachaidan gabbros formed in a forearc setting. Previous studies have suggested that forearc tholeiites form during subduction initiation and the transition to a continental setting (Xiao et al., 2016). Therefore, the Dachaidan gabbros were the products of intra-oceanic subduction at the northern margin of the North Qaidam Ocean.

5.5 Geodynamic processes

The NQUB contains granitic gneiss, pelitic gneiss, and sporadic occurrences of eclogite and garnet clinopyroxenite. It also contains island arc ophiolitic mélange, and collisional and post-collisional granites (Wu et al., 2004; Wu et al., 2007; Wu et al., 2008; Wu et al., 2014; Zhu et al., 2010; Zhu et al., 2012; Zhu et al., 2014; Song et al., 2015; Zhao et al., 2017). The rock assemblages associated with the eclogites suggest that the UHP metamorphic zone in the NQUB is typical of an early Paleozoic continental orogenic belt (Ren et al., 2019). Some eclogites have geochemical characteristics typical of oceanic basalts, indicative of derivation from either middle

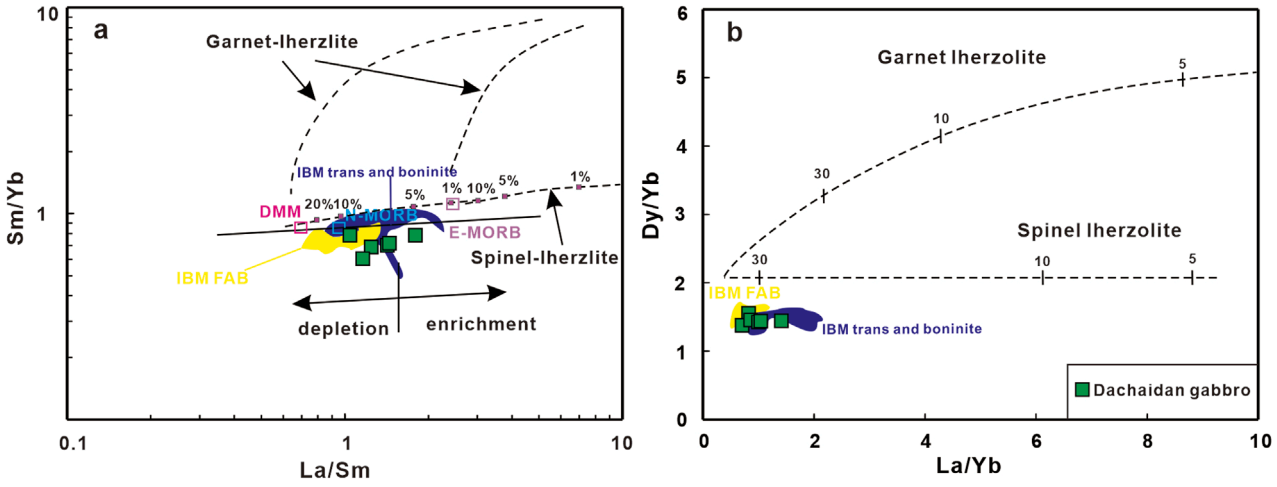

FIGURE 9
(A) La/Sm–Sm/Yb (Kinzler, 1994) and **(B)** La/Yb–Dy/Yb diagrams showing the effects of source lithology, degree of partial melting, and REE composition of the mantle source. Data for the IBM forearc basalts are from Reagan et al., 2010.

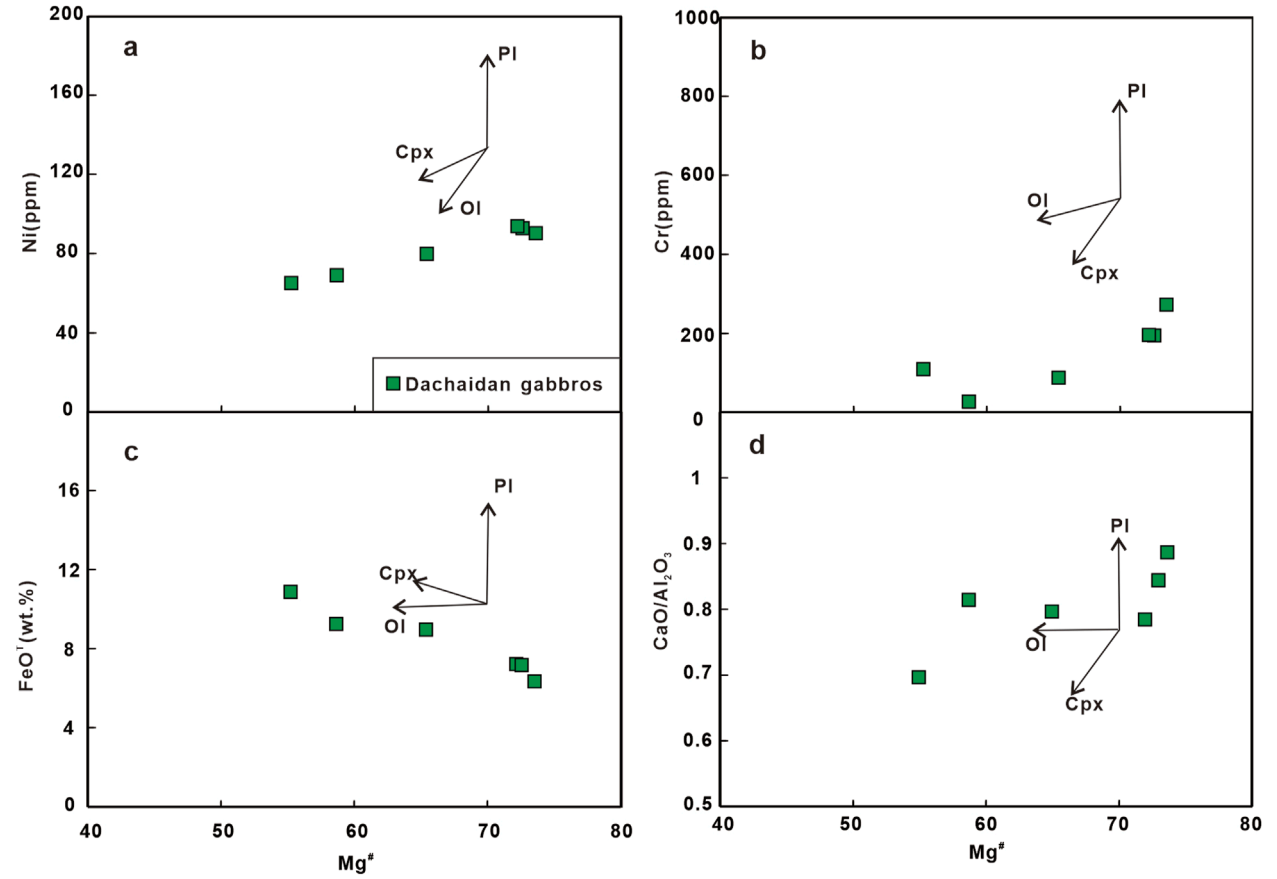

FIGURE 10
PPlots of selected major and trace elements versus Mg$^{\#}$ values for the Dachaidan gabbros **(A-D)** (modified after Yao et al., 2012).

Proterozoic oceanic crust, as is the case for the Shaliuhe section in the South Dulan belt. This section consists of blueschist garnet, phengite–garnet, and epidote–garnet eclogites with the protolith ages from 1,280 to 1,070 Ma, the protolith may be Mesoproterozoic oceanic crust and a peak metamorphic age of 439–430 Ma (Ren et al., 2019). Alternatively, these rocks may have been derived from early Paleozoic oceanic crust, as exemplified by the blueschist garnet eclogites from the Shaliuhe area, the protolith of these

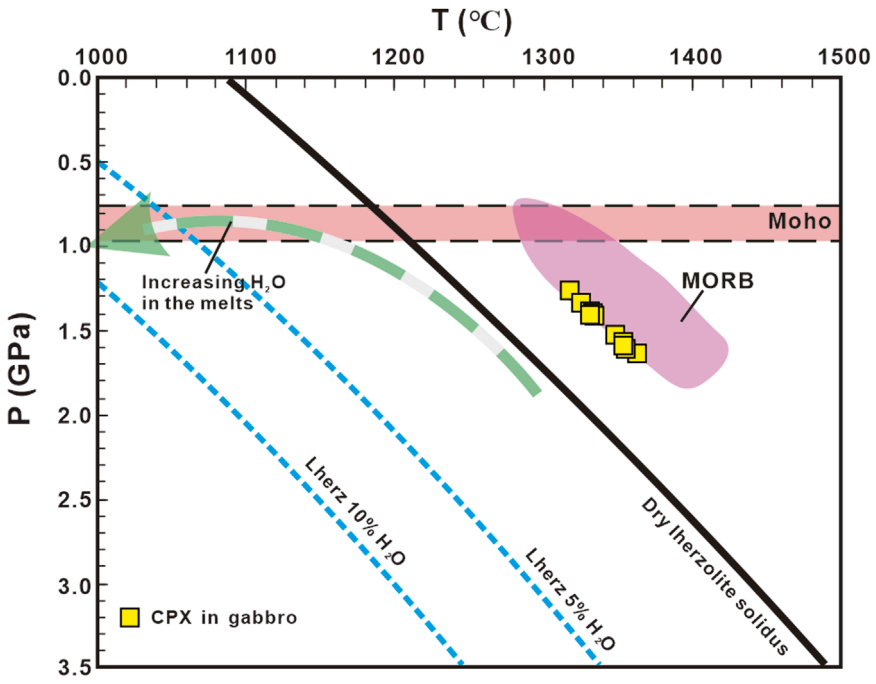

FIGURE 11
Temperatures and pressures obtained by clinopyroxene geothermobarometry for the Dachaidan gabbros. The purple field represents the temperatures and pressures calculated for MORBs (data from Lee et al., 2009).

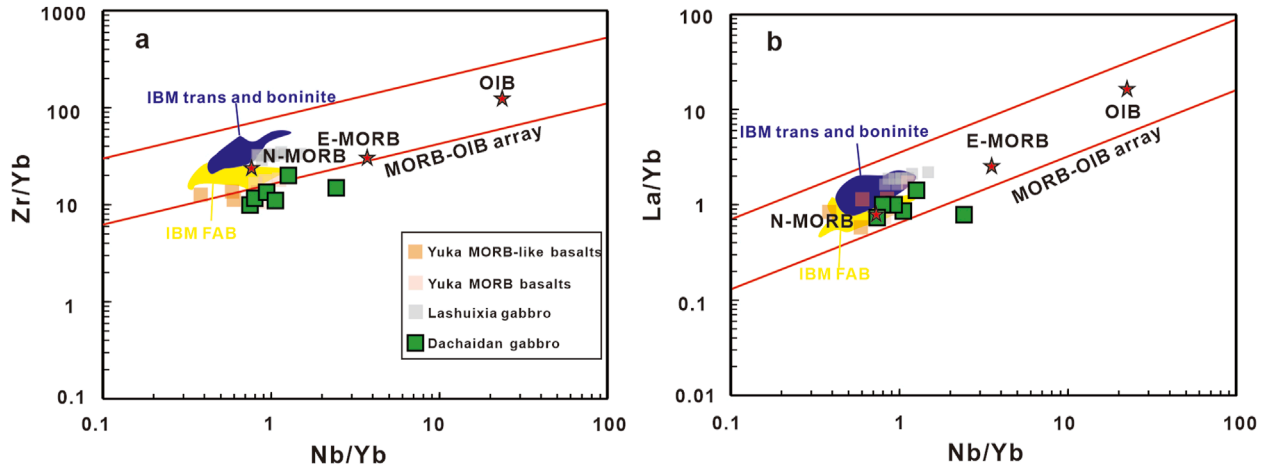

FIGURE 12
Plots of trace element ratios for the Dachaidan gabbros **(A,B)** (Yuka MORB-like and MORB data are from Zhu, 2021; Lashuixia gabbro data are from Lu et al., 2018). Data for the IBM forearc basalts are from Reagan et al., 2010.

eclogites ages formed at 517–514 Ma and peak metamorphic ages of 457–440 Ma (Zhang et al., 2009a; Zhang et al., 2009b; Zhang et al., 2016). These findings provide insights into the presence of an early Cambrian Proto-Tethyan oceanic basin. In summary, the geological investigations of the NQUB revealed a complex tectonic history involving continental collision and the presence of an early Cambrian Proto-Tethyan oceanic basin.

Song et al. (2014b) investigated the northern Qilian region and NQUB, where oceanic-type eclogites with a peak metamorphic age of 489–464 Ma were previously identified (Song et al., 2006). This age is similar to the metamorphic age of oceanic eclogites in the NQUB, leading to the conclusion that the northern Qilian region and NQUB are part of the same geological system. The continental-type, UHP metamorphic belt in the NQUB formed by northward subduction that caused the Qilian–NQUB block to undergo continental subduction. The UHP metamorphic rocks in the belt are considered to have formed by either exhumation along the subduction path or exhumation through bottom-driven

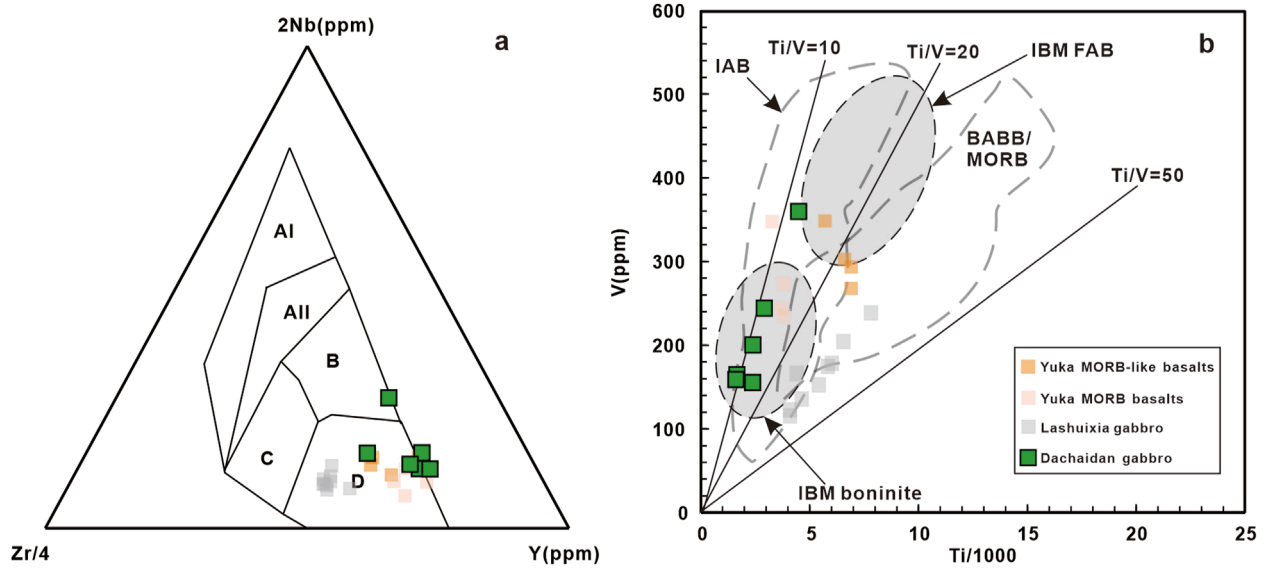

FIGURE 13
(A) 2Nb–Zr/4–Y tectonic setting discrimination diagram (after Meschede, 1986) and **(B)** V–Ti/1000 diagram (after Shervais, 1982) for the Dachaidan gabbros (Yuka MORB-like and MORB data are from Zhu, 2021; Lashuixia gabbro data are from Lu et al., 2018). AI, within-plate alkaline basalt; AII, within-plate alkaline and tholeiitic basalts; B, enriched MORB; C, intraplate tholeiitic basalt; D, N-MORB and volcanic arc basalt; IAB, island arc basalt; MORB, mid-ocean ridge basalt; OIB, ocean island basalt.

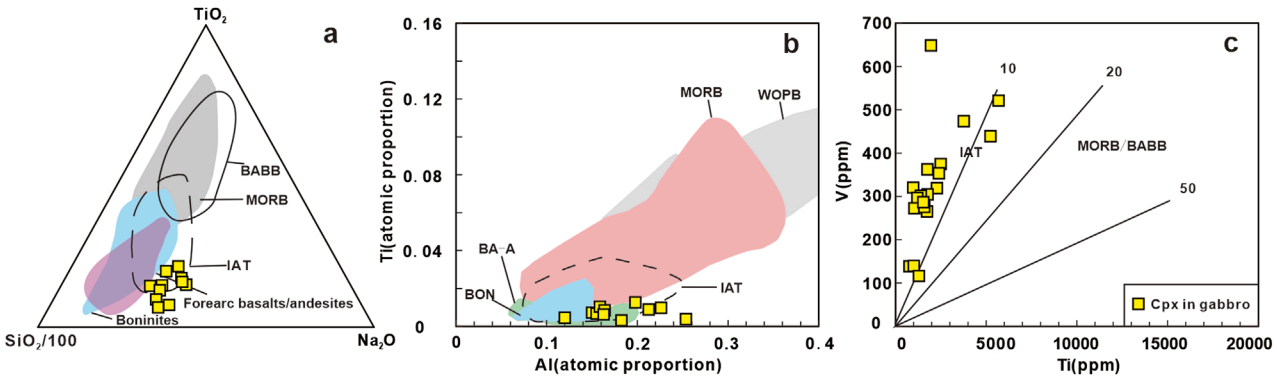

FIGURE 14
Tectonic discrimination diagrams for clinopyroxenes from the Dachaidan gabbros. **(A)** TiO_2–SiO_2/100–Na_2O (Beccaluva et al., 1989). **(B)** Atomic Ti versus Al (Beccaluva et al., 1989). **(C)** Ti versus V (Shervais, 1982). BON, boninite; BA-A, back-arc andesite; IAT, island arc tholeiite; MORB, mid-ocean ridge basalt; WOPB, within-oceanic plate basalt; BABB, back-arc basin basalt.

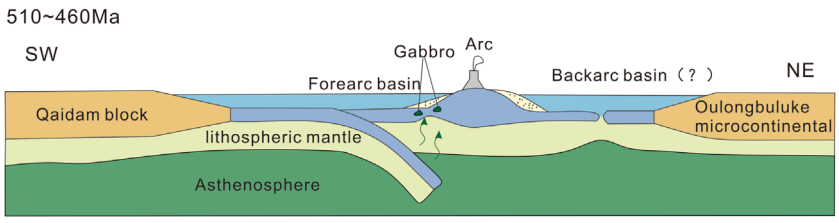

FIGURE 15
Schematic diagram of the early Paleozoic tectonic evolution of the NQOB (modified after Cai et al., 2021).

uplift (Song et al., 2006; Song et al., 2014b; Yin et al., 2007). MORB-type ophiolites in the NQUB include the Dulan–Shaliuhe section dated at 520 Ma (Wang et al., 2020) and the Amunike ophiolite dated at 485.6 Ma (Li et al., 2018). In addition, some mafic igneous rocks within the intercalated island arc mélange of the NQUB had diverse tectonic settings, such as island arc, back-arc basin, ocean island, and mid-ocean ridge environments. These include the 521 Ma Xitieshan OIB-type basalts (Zhu et al., 2012), 480 Ma Tuomoerite N-MORB-type basalts (Wang et al., 2022), and 542–460 Ma island arc volcanic rocks (Yuan et al., 2002; Shi et al., 2003; Wang et al., 2023; Wang et al., 2005; Zhu et al., 2010, Zhu et al., 2012; Zhu et al., 2014; Gao et al., 2011). These features are similar to those of early Paleozoic oceanic eclogites in the Dulan region, which protolith age is 510 ± 19 Ma (Zhang et al., 2009a; Zhang et al., 2009b; Zhang G. B. et al., 2016). Consequently, we infer that there was an independent ocean (i.e., the North Qaidam Ocean) in the region during the early Paleozoic, and that the northern Qilian region and NQUB should not be considered to have been a single entity.

Geochronological studies have revealed that the eclogites in the Xitieshan experienced peak metamorphism at 458–420 Ma (Chen et al., 2012; Liu et al., 2012; Zhang et al., 2013b; Zhang L. et al., 2016). The subordinate gneisses in the Xitieshan underwent prograde metamorphism from 460 to 455 Ma, followed by retrograde metamorphism at 425–422 Ma (Zhang et al., 2012). The metamorphic ages of quartz diorites and eclogites intercalated with the subordinate gneisses in the Dulan region are 458–421 Ma (Yang et al., 2005; Chen et al., 2008). Blueschist garnet eclogites in the Shaliuhe area have peak metamorphic ages of 457–440 Ma (Zhang et al., 2009a; Zhang et al., 2009b; Zhang G. B. et al., 2016). All these ages indicate that subduction in the North Qaidam Ocean started at *ca.* 460 Ma and persisted until *ca.* 421 Ma. Given the oceanic nature of these rocks, this study suggests the Dachaidan gabbros were formed in an intra-oceanic forearc environment. The zircon U–Pb age of 510 Ma indicates subduction in the North Qaidam Ocean started prior to 510 Ma.

We propose the early Paleozoic tectonic evolution of the NQUB was as follows. During 510–460 Ma, the North Qaidam Ocean existed between the Qaidam Block and Oulongbuluke micro-continent. Subsequently, the ocean experienced northward subduction (Figure 15A), which led to the development of a forearc ophiolite in the Dachaidan region, a back-arc basin ophiolite in the Tuomoerrite Basin, and other related features. The present-day NQUB ophiolite is considered to comprise remnants of the oceanic crust.

6 Conclusion

(1) The age of the Dachaidan gabbros is 510.0 ± 2.9 Ma and 510.0 ± 2.8 Ma, indicating the ophiolite in the region formed during the early Cambrian.
(2) The Dachaidan gabbros formed by decompression partial melting of depleted mantle.
(3) The Dachaidan gabbros have the geochemical characteristics of both island arc volcanic rocks and MORBs, indicating the northern margin of the Qaidam Basin was in an oceanic subduction setting during the early Cambrian.

Data availability statement

The original contributions presented in the study are included in the article/Supplementary Material, further inquiries can be directed to the corresponding author.

Author contributions

YQ: Writing–original draft, Writing–review and editing. XjL: Funding acquisition, Writing–review and editing. XaL: Investigation, Writing–review and editing. QH: Resources, Writing–review and editing. QY: Data curation, Writing–review and editing. RH: Formal Analysis, Writing–review and editing. PL: Formal Analysis, Writing–review and editing. YS: Formal Analysis, Writing–review and editing.

Funding

The author(s) declare that financial support was received for the research, authorship, and/or publication of this article. Financial support for this research was provided by the National Natural Science Foundation of China (No. 92055208), and the Guangxi Science Innovation Base Construction Foundation (No. GuikeZY21195031), the Natural Science Foundation of Guangxi Province for Young Scholars (No. GuikeAD23026175). This research is a contribution to "Xinjiang Tianchi Distinguished Expert" by Xi-Jun Liu.

Conflict of interest

The authors declare that the research was conducted in the absence of any commercial or financial relationships that could be construed as a potential conflict of interest.

Publisher's note

All claims expressed in this article are solely those of the authors and do not necessarily represent those of their affiliated organizations, or those of the publisher, the editors and the reviewers. Any product that may be evaluated in this article, or claim that may be made by its manufacturer, is not guaranteed or endorsed by the publisher.

Supplementary material

The Supplementary Material for this article can be found online at: https://www.frontiersin.org/articles/10.3389/feart.2024.1473101/full#supplementary-material

References

Beccaluva, L., Macciotta, G., Piccardo, G. B., and Zeda, O. (1989). Clinopyroxene composition of ophiolite basalts as petrogenetic indicator. *Chem. Geol.* 77, 165–182. doi:10.1016/0009-2541(89)90073-9

Brown, G. (1967). *Mineralogy of the basaltic rocks*. Editors H. H. Hess, and A. Poldervaart (New York, NY: Basalts. Interscience).

Cai, P. J., Chen, X., Majka, J., Klonowska, I., Jeanneret, P., Xu, R. K., et al. (2021). Two stages of crust-mantle interaction during oceanic subduction to continental collision: insights from mafic-ultramafic complexes in the North Qaidam orogen. *Gondwana Res.* 89, 247–264. doi:10.1016/j.gr.2020.08.018

Carracedo, J. (1999). Growth, Structure, instability and collapse of Canarian volcanoes and comparisons with Hawaiian volcanoes. *J. Volcanol. Geoth Res.* 94 (1-4), 1–19. doi:10.1016/S0377-0273(99)00095-5

Chen, D. L., Liu, L., Sun, Y., and Liou, J. G. (2009). Geochemistry and zircon U–Pb dating and its implications of the Yukahe HP/UHP terrane, the North Qaidam, NW China. *J. Asian Earth Sci.* 35, 259–272. doi:10.1016/j.jseaes.2008.12.001

Chen, D. L., Liu, L., Sun, Y., Sun, W. D., Zhu, X. H., Liu, X. M., et al. (2012). Felsic veins within UHP eclogite at xitieshan in North Qaidam NW China: partial melting during exhumation. *Lithos* 136, 187–200. doi:10.1016/j.lithos.2011.11.006

Chen, D. L., Sun, Y., and Liu, L. (2007). The metamorphic ages of the country rocks of the yukahe eclogites in the northern margin of Qaidam Basin and its geological significance. *EarthScience Front.* 14 (1), 108–116. (in Chinese with English abstract). doi:10.1016/s1872-5791(07)60005-0

Chen, D. L., Sun, Y., and Liu, L. (2008). Zircon U-Pb Dating of paragneiss interbed in the UHP eclogite from Yematan area, the North Qaidam UHP terrane, NW China. *Acta Petrol Sin.* 24, 1059–1067. (in Chinese with English abstract).

Cheng, Y. H., Zhang, T. F., Li, Y. F., Li, M., Niu, W. C., Teng, X. J., et al. (2016). Discovery of the early permian ultramafic rocks in dongujimqi, inner Mongolia and its tectonic tmplications. *Acta Geol. Sin.* 90, 115–125. (in Chinese with English abstract). doi:10.3969/j.issn.0001-5717.2016.01.007

Condie, K. (1989). Geochemical changes in baslts and andesites across the Archean-Proterozoic boundary: identification and significance. *Lithos* 23 (1-2), 1–18. doi:10.1016/0024-4937(89)90020-0

Dong, Z. C., Gu, P. Y., Jiao, H., Zha, X. F., Chen, R. M., and Zhang, H. D. (2014). Geochemistry and Geochronology of Yanchangbeishan gabbro in Lenghu area at the west segment of the north margin of Qaidam. *Geol. Sci.* 49, 1132–1149. (in Chinese with English abstract). doi:10.3969/j.issn.0563-5020.2014.04.007

Escuder, P., Pérez-Estaún, A., Weis, D., and Friedman, R. (2010). Geochemical characteristics of the río verde complex central hispaniola: implications for the paleotectonic reconstruction of the lower cretaceous caribbean island-arc. *Lithos* 114, 168–185. doi:10.1016/j.lithos.2009.08.007

Gao, W. L., Wang, Z. X., Li, L. L., Cui, M. M., Qian, T., and Hu, J. J. (2019). Discovery of the Permian granite in saishiteng Mountain of the Northern Qaidam basin and its tectonic significance. *Acta Geol. Sin.* 93, 816–829. (in Chinese with English abstract).

Gao, X. F., Xiao, P. X., and Jia, Q. Z. (2011). Redetermination of the TanjianShan group: geochronological and geochemical evidence of basalts from the margin of the Qaidam Basin. *Acta Geol. Sin.* 85, 1452–1463. (in Chinese with English abstract).

Hajash, A. (1984). Rare earth element abundances and distribution patterns in hydrothermally altered basalts: experimental results. *Contrib. Mineral. Petr* 85, 409–412. doi:10.1007/bf01150297

Hao, G. J., Lu, S. N., Li, H. K., and Zheng, J. K. (2001). Determination and significant of eclogite on Shaliuhe, in the North margin of Qaidam basin. *Precambrian Res.* 3, 154–162. (in Chinese with English abstract). doi:10.3969/j.issn.1672-4135.2001.03.003

Hart, S. (1984). A large-scale isotope anomaly in the Southern Hemisphere mantle. *Nature* 309, 753–757. doi:10.1038/309753a0

Hoskin, P. W., and Black, L. P. (2000). Metamorphic zircon formation by solid-state recrystallization of protolith igneous zircon. *Journal of Metamorphic Geol.* 18, 423–439.

Ishizuka, O., Tani, K., and Reagan, M. K. (2014). Izu-Bonin-Mariana forearc crust as a modern ophiolite analogue. *Elements* 10 (2), 115–120. doi:10.2113/gselements.10.2.115

Kersting, A. B., and Arculus, R. J. (1994). Pb isotope composition of Klyuchevskoy volcano, Kamchatka and North Pacific sediments: implications for magma genesis and crustal recycling in the Kamchatkan arc. *Mineral. Mag.* 136, 133–148. doi:10.1016/0012-821x(95)00196-j

Kinzler, R. (1994). Melting of mantle peridotite at pressures approaching the spinel to garnet transition. *Mineral. Mag.* 102, 483–484. doi:10.1180/minmag.1994.58a.1.251

Langmuir, C. H., Bender, J. F., Bence, A. E., Hanson, G. N., and Taylor, S. R. (1977). Petrogenesis of basalts from the FAMOUS area: mid-Atlantic Ridge. *Earth Planet Sci. Lett.* 36, 133–156. doi:10.1016/0012-821X(77)90194-7

Lee, C. A., Luffi, P., Plank, T., Dalton, H., and Leeman, W. P. (2009). Constraints on the depths and temperatures of basaltic magma generation on Earth and other terrestrial planets using new thermobarometers for mafic magmas. *Earth Planet Sci Lett* 279 (1-2), 20–33. doi:10.1016/j.epsl.2008.12.020

Leterrier, J., Maury, R. C., Thonon, P., Girard, D., and Marchal, M. (1982). Clinopyroxene composition as a method of identification of the magmatic affinities of paleo-volcanic series. *Earth Planet Sci Lett* 59, 139–154. doi:10.1016/0012-821X(82)90122-4

Li, J. B., Meng, J. H., and Wan, S. C. (2018). The discovery and geological significance of the northern Amunike ophiolitic melange in the northern Qaidam basin. *Xinjiang Geol.* 36, 386–392. (in Chinese with English abstract).

Li, X. H., Li, W. X., Wang, X. C., Li, Q. L., Liu, Y., and Tang, G. Q. (2009). Role of mantle-derived magma in genesis of early Yanshanian granites in the Nanling Range South China: *in situ* zircon Hf-O isotopic constraints. *Sci. China Ser. D Earth Sci.* 52, 1262–1278. doi:10.1007/s11430-009-0117-9

Li, Y. W., Deng, J. F., Luo, Z. H., Zeng, Z. P., Cao, Y. Q., and Luo, F. (1995). Discovery and geological significance of cumulate hornblende diorite in sunit left banner inner Mongolia. *Geosci* 9, 212–219. (in Chinese with English abstract).

Lin, C. L., Sun, Y., Chen, D. L., and Di, W. C. R. (2006). Geochemistry and zircon LA-ICPMS dating of iqe river granite gneiss, northern margin of Qaidam Basin. *Geochemistry*, 489–505. (in Chinese with English abstract).

Liotard, J. M., Briot, D., and Boivin, P. (1988). Petrological and geochemical relationships between pyroxene megacrysts and associated alkali-basalts from Massif Central (France). *Contrib Mineral Petr* 98, 81–90. doi:10.1007/bf00371912

Liu, X. C., Wu, Y. B., Gao, S., Liu, Q., Wang, H., Qin, Z. W., et al. (2012). First record and timing of UHP metamorphism from zircon in the Xitieshan terrane: implications for the evolution of the entire North Qaidam metamorphic belt. *Am. Mineral.* 97, 1083–1093. doi:10.2138/am.2012.4048

Liu, X. J., Xu, J. F., Castillo, P. R., Xiao, W. J., Shi, Y., Zhang, Z. G., et al. (2021). Long-lived low Th/U Pacific-type isotopic mantle domain: constraints from Nd and Pb isotopes of the Paleo-Asian Ocean mantle. *Earth Planet Sci. Lett.* 567, 117006. doi:10.1016/j.epsl.2021.117006

Lu, T., Zhang, H. F., Yang, H., Gao, Z., Pan, F. B., and Luo, B. J. (2018). Initial back-arc extension: evidence from petrogenesis of early Paleozoic MORB-like gabbro at the southern Central Qilian block NW China. *Lithos* 322, 166–178. doi:10.1016/j.lithos.2018.10.015

McCulloch, M. T., Gregory, R. T., Wasserburg, G. J., and Taylor, H. P. (1980). A neodymium strontium and oxygen isotopic study of the Cretaceous Samail ophiolite and implications for the petrogenesis and seawater-hydrothermal alteration of oceanic crust. *Earth Planet Sci. Lett.* 46, 201–211. doi:10.1016/0012-821X(80)90006-0

McCulloch, M. T., Gregory, R. T., Wasserburg, G. J., and Taylor, H. P. (1981). Sm-Nd, Rb-Sr, and $^{18}O/^{16}O$ isotopic systematics in an oceanic crustal section: evidence from the samail ophiolite. *J. Geophys Res.* 86, 2721–2735. doi:10.1029/jb086ib04p02721

Meng, F. C., Zhang, J. X., Yang, J. S., and Xu, Z. Q. (2003). Geochemical characteristics of eclogites in xitieshan area, North Qaidam of northwestern China. *Acta Petrol Sin.* 19 (3), 435–442. (in Chinese with English abstract). doi:10.3969/j.issn.1000-0569.2003.03.007

Meschede, M. (1986). A method of discriminating between different types of mid-ocean ridge basalts and continental tholeiites with the Nb-1bZr-1bY diagram. *Chem. Geol.* 56, 207–218. doi:10.1016/0009-2541(86)90004-5

Pearce, J. A., Harris, N. B., and Tindle, A. G. (1984). Trace element discrimination diagrams for the tectonic interpretation of granitic rocks. *J. Petrol* 25, 956–983. doi:10.1093/petrology/25.4.956

Pearce, J. A., and Peate, D. W. (1995). Tectonic implications of the composition of volcanic arc magmas. *Annu. Rev. Earth Planet. Sci.* 23, 251–285. doi:10.1146/annurev.ea.23.050195.001343

Philpotts, J. A., Schnetzler, C. C., and Hart, S. R. (1969). Submarine basalts: some K, Rb, Sr, Ba, rare-earth, H_2O, and CO_2 data bearing on their alteration, modification by plagioclase, and possible source materials. *Earth. Plane. Sci.* 7 (3), 293–299. doi:10.1016/0012-821x(69)90068-5

Putirka, K. D. (2008). Thermometers and barometers for volcanic systems. *Rev mineral geochem* 25, 61–120. doi:10.2138/rmg.2008.69.3

Reagan, M. K., Ishizuka, O., Stern, R. J., Kelley, K. A., Ohara, Y., Blichert-Toft, J., et al. (2010). Fore-arc basalts and subduction initiation in the Izu-Bonin-Mariana system. *Geochem. Geophys. Geosyst.* 11, 1–17. doi:10.1029/2009gc002871

Ren, Y. F., Chen, D. L., Wang, H. J., Zhu, X. H., Bai, B. W., Kong, H. X., et al. (2022). Origin and metamorphic evolution of Chachahe eclogites North Qaidam UHP metamorphic Belt NW China: implications for fate of overriding plate material in subduction channel. *J. Asian Earth Sci.* 236, 105331. doi:10.1016/j.jseaes.2022.105331

Ren, Y. F., Chen, D. L., Zhu, X. H., Ren, Z. L., Gong, X. K., and Luo, F. H. (2019). Two orogenic cycles recorded by eclogites in the Yuka–Luofengpo terrane: implications for the Mesoproterozoic to early Paleozoic tectonic evolution of the North Qaidam orogenic belt NW China. *Precambrian Res.* 333, 105449. doi:10.1016/j.precamres.2019.105449

Saunders, A. D., Norry, M. J., and Tarney, J. (1988). Origin of MORB and chemically-depleted mantle reservoirs: trace element constraints. *J. Petrol Special_* Volume (1), 415–445. doi:10.1093/petrology/special_volume.1.415

Shervais, J. W. (1982). Ti-V plots and the petrogenesis of modern and ophiolitic lavas. *Earth Planet Sci. Lett.* 59, 101–118. doi:10.1016/0012-821X(82)90120-0

Shi, R. D., Yang, J. S., and Wu, C. L. (2003). The discovery of adakitic dacite in Early Paleozoic arc volcanic rocks on the Northern Qaidam Basin and its geological significant. *Acta Petrol Mineral* 3, 229–236. (in Chinese with English abstract). doi:10.3969/j.issn.1000-6524.2003.03.004

Song, S. G., Niu, Y. L., Su, L., Wei, C. J., and Zhang, L. F. (2014b). Adakitic (tonalitic-trondhjemitic) magmas resulting from eclogite decompression and dehydration melting during exhumation in response to continental collision. *Geochimi Cosmochim. Acta* 130, 42–62. doi:10.1016/j.gca.2014.01.008

Song, S. G., Niu, Y. L., Su, L., and Xia, X. H. (2013). Tectonics of the North qilian orogen NW China. *Gondwana Res.* 23, 1378–1401. doi:10.1016/j.gr.2012.02.004

Song, S. G., Niu, Y. L., Su, L., Zhang, C., and Zhang, L. F. (2014a). Continental orogenesis from ocean subduction continent collision/subduction to orogen collapse and orogen recycling: the example of the North Qaidam UHPM belt NW China. *Earth-Sci Rev.* 129, 59–84. doi:10.1016/j.earscirev.2013.11.010

Song, S. G., Niu, Y. L., Zhang, G. B., and Zhang, L. F. (2019). Two epochs of eclogite metamorphism link 'cold' oceanic subduction and 'hot' continental subduction the North Qaidam UHP belt NW China. *Geol. Soc. Lond Spec. Publ.* 474, 275–289. doi:10.1144/sp474.2

Song, S. G., Su, L., Li, X. H., Zhang, G. B., Niu, Y. L., and Zhang, L. F. (2010). Tracing the 850Ma continental flood basalts from a piece of subducted continental crust in the North Qaidam UHPM belt NW China. *Precambrian Res.* 183, 805–816. doi:10.1016/j.precamres.2010.09.008

Song, S. G., Wang, M. J., Wang, C., and Niu, Y. L. (2015). Magmatism during continental collision, subduction, exhumation and mountain collapse in collisional orogenic belts and continental net growth: A perspective. *Sci. China Earth Sci.* 45 (07), 916–940. (in Chinese with English abstract)

Song, S. G., and Yang, J. S. (2001). Sanidine+Quartz inclusions in dulan eclogites: evidence from UHP metamorphism on the North margin of the Qaidam Basin, NW China. *Acta Geol. Sin. 02*, 180–185. (in Chinese with English abstract). doi:10.3321/j.issn:0001-5717.2001.02.006

Song, S. G., Zhang, L. F., and Niu, Y. L. (2004b). Ultra-deep origin of garnet peridotite from the North Qaidam ultrahigh-pressure belt Northern Tibetan Plateau NW China. *Am. Mineral.* 89 (8-9), 1330–1336. doi:10.2138/am-2004-8-922

Song, S. G., Zhang, L. F., Niu, Y. L., Song, B., and Liu, D. Y. (2004a). Early Paleozoic plate tectonic evolution and continental subduction on the Northern margin of the Qinghai-Tibetan Plateau. *Geol. Bull. China* Z2, 918–925. (in Chinese with English abstract). doi:10.3969/j.issn.1671-2552.2004.09.014

Song, S. G., Zhang, L. F., Niu, Y. L., Su, L., Song, B., and Liu, D. (2006). Evolution from oceanic subduction to continental collision: a case study from the Northern Tibetan Plateau based on geochemical and geochronological data. *J. Petrol* 47, 435–455. doi:10.1093/petrology/egi080

Stille, P., Unruh, D. M., and Tatsumoto, M. (1983). Pb-Sr-Nd and Hf isotopic evidence of multiple sources for Oahu Hawaii basalts. *Nature* 304, 25–29. doi:10.1038/304025a0

Stracke, A., Bizimis, M., and Salters, V. (2003). Recycling oceanic crust: quantitative constraints. *Geochem. Geophys. Geosyst.* 4, 8003. doi:10.1029/2001GC000223

Sun, G. C. (2020). *Remobilization and recycling of subducted crustal material: geochemical evidence from paleozoic magmatic rocks in the northern chai region*. Dissertation: University of Science and Technology of China. (in Chinese with English abstract).

Sun, S. S., and Nesbitt, R. W. (1978). Geochemical regularities and genetic significance of ophiolitic basalts. *Geol* 6 (11), 689–693. doi:10.1130/0091-7613(1978)6<689:gragso>2.0.co;2

Sun, W. D., and McDonough, W. (1989). Chemical and isotopic systematics of oceanic basalts: implications for mantle composition and processes. *Geol. Soc. Lond Spec. Publ.* 42 (1), 313–345. doi:10.1144/gsl.sp.1989.042.01.19

Tian, L. Y., Castillo, P. R., Hawkins, J. W., Hilton, D. R., Hanan, B. B., and Pietruszka, A. J. (2008). Major and trace element and Sr–Nd isotope signatures of lavas from the Central Lau Basin: implications for the nature and influence of subduction components in the back-arc mantle. *J. Volcanol. Geoth Res.* 178, 657–670. doi:10.1016/j.jvolgeores.2008.06.039

Tung, K. A., Yang, H. Y., Liu, D. Y., Zhang, J. X., Yang, H. J., Shau, Y. H., et al. (2012). The amphibolite-facies metamorphosed mafic rocks from the Maxianshan area Qilian block NW China: a record of early Neoproterozoic arc magmatism. *J. Asian Earth Sci.* 46, 177–189. doi:10.1016/j.jseaes.2011.12.006

Tung, K. A., Yang, H. Y., Liu, D. Y., Zhang, J. X., Yang, H. J., Shau, Y. H., et al. (2013). The neoproterozoic granitoids from the qilian block NW China: evidence for a link between the qilian and South China blocks. *Precambrian Res.* 235, 163–189. doi:10.1016/j.precamres.2013.06.016

Tuo, Y. (2019). *Records of early Paleozoic ocean activities in the North Qaidam—contraints from Kaipinggou ophiolite*. Dissertation. Northwest University. (in Chinese with English abstract).

Wang, H. C., Lu, S. N., Mo, X. X., Li, H. K., and Xin, H. T. (2005). An early paleozoic collisional orogeny on the northern margin of the Qaidam Basin, northwestern China. *Geol. Bull. China 07*, 603–612+11. (in Chinese with English abstract). doi:10.3969/j.issn.1671-2552.2005.07.003

Wang, H. C., Yuan, G. B., Xin, H. T., Hao, G. J., Zheng, J. K., and Zhang, B. H. (2001). Preliminary study on outcrop and origin of gneiss in green liangshan area North Qaidam. *Chin. Geol.* 28, 22–27+28. (in Chinese with English abstract).

Wang, J. X., Lin, M., Liu, Z. Y., Wang, L., and Zhang, G. B. (2020). Petrological study of the meta-ophiolite from the North Qaidam UHP Belt and its geological implications. *Northwest. Geol.* 53, 1–10. (in Chinese with English abstract).

Wang, X. D., Ding, L., Zeng, D., Yue, Y. H., Yang, L. P., Wang, Z. J., et al. (2023). Protolith origin of eclogites from the North Qaidam UHP metamorphic belt NW China: implications for the breakup of the Rodinia supercontinent. *Precambrian Res.* 384, 106942. doi:10.1016/j.precamres.2022.106942

Wang, Z. Q., Zhang, Z. W., Ding, P. C., Feng, J. Z., Xue, Z. Q., and Lu, D. X. (2022). Geochronology, geochemistry and significance of metabasic volcanic rocks in Tuomoerrite area, North Qaidam. *J. Petro Mineral.* 41, 491–503. (in Chinese with English abstract). doi:10.3969/j.issn.1000-6524.2022.03.001

Winchester, J. A., and Floyd, P. A. (1977). Geochemical discrimination of different magma series and their differentiation products using immobile elements. *Chem. Geol.* 20, 325–343. doi:10.1016/0009-2541(77)90057-2

Wu, C. L., Gao, Y. H., Li, Z. L., Lei, M., Qin, H. P., Li, M. Z., et al. (2014). Zircon SHRIMP dating of granitic rocks and chronostratigraphic framework of UHP rocks in the northern Qaidam Basin. *Sci. China Earth Sci.* 44, 2142–2165. (in Chinese with English abstract).

Wu, C. L., Gao, Y. H., Wu, S. P., Chen, Q. L., Wooden, J. L., Mazdab, F. K., et al. (2008). Zircon SHRIMP U-Pb dating and petrogeochemistry of granites in the western Qaidam inner Mongolia. Sci China. *Earth Sci.* 08, 930–949+10+14. (in Chinese with English abstract).

Wu, C. L., Yang, J. S., Xu, Z. Q., Wooden, J. L., Li, H. B., Shi, R. D., et al. (2004). Granitic magmatism in the early paleozoic UHP belt of the North Qaidam. *Acta Geol. Sin.* 658-674. (in Chinese with English abstract). doi:10.3321/j.issn:0001-5717.2004.05.010

Wu, F. Y., Li, X. H., Zheng, Y. F., and Gao, S. (2007). Lu-Hf isotope systematics and their applications in petrology. *Acta Petrol Sin.* 02, 185–220. (in Chinese with English abstract). doi:10.3321/j.issn:1000-0569.2007.02.001

Xiao, W. J., Windley, B. F., Yong, Y., Yan, Z., Yuan, C., Liu, C. Z., et al. (2009). Early paleozoic to devonian multiple-accretionary model for the qilian Shan NW China. *J. Asian Earth Sci.* 35, 323–333. doi:10.1016/j.jseaes.2008.10.001

Xiao, Q. H., Li, T. D., Pan, G. T., Lu, S. N., Ding, X. Z., Deng, J. F., et al. (2016). Petrologic ideas for identification of ocean-continent transition: Recognition of intra-oceanic arc and initial subduction. *China Geol.* 43 (03), 721–737. (in Chinese with English abstract).

Xu, J. F., Castillo, P. R., Chen, F. R., Niu, H. C., Yu, X. Y., and Zhen, Z. P. (2003). Geochemistry of late Paleozoic mafic igneous rocks from the Kuerti area Xinjiang northwest China: implications for backarc mantle evolution. *Chem. Geol.* 193, 137–154. doi:10.1016/S0009-2541(02)00265-6

Xu, Z. Q., Yang, J. S., Wu, C. L., Li, H. B., Zhang, J. X., Qi, X. X., et al. (2006). Timing and mechanism of formation and exhumation of the Northern Qaidam ultrahigh-pressure metamorphic belt. *J. Asian Earth Sci.* 28, 160–173. doi:10.1016/j.jseaes.2005.09.016

Yan, Z., Aitchison, J., Fu, C. L., Guo, X. Q., Niu, M. L., Xia, W. J., et al. (2015). Hualong Complex South Qilian terrane: U–Pb and Lu–Hf constraints on Neoproterozoic micro-continental fragments accreted to the northern Proto-Tethyan margin. *Precambrian Res.* 266, 65–85. doi:10.1016/j.precamres.2015.05.001

Yang, J. H., Sun, J. F., Chen, F. K., Wilde, S. A., and Wu, F. Y. (2007). Sources and petrogenesis of late triassic dolerite dikes in the liaodong peninsula: implications for post-collisional lithosphere thinning of the eastern north China craton. *J. Petrol* 48, 1973–1997. doi:10.1093/petrology/egm046

Yang, J. S., Liu, F. L., Wu, C. L., Xu, Z. Q., Shi, R. D., Chen, S. Y., et al. (2005). Two ultrahigh-pressure metamorphic events recognized in the central orogenic belt of China: evidence from the U-Pb dating of coesite-bearing zircons. *Int. Geol. Rev.* 47, 327–343. doi:10.2747/0020-6814.47.4.327

Yang, J. S., Song, S. G., Xu, Z. Q., Wu, C. L., Shi, R. D., Zhang, J. X., et al. (2001). Discovery of coesite in the North Qaidam early Paleozoic Ultrahigh-high pressure(UHP-HP) metamorphic belt, NW China. *Acta Geol. Sin. 02*, 175–179+35. (in Chinese with English abstract).

Yang, J. S., Xu, Z. Q., Li, H. B., Wu, C. L., Cui, J. W., Zhang, J. X., et al. (1998). *Discovery of eclogite in the North Qaidam western China*. Chinese Sci Bull, 1544–1549. (in Chinese with English abstract).

Yang, L. M., Song, S. G., Su, L., Allen, M. B., Niu, Y. L., Zhang, G. B., et al. (2019). Heterogeneous oceanic arc volcanic rocks in the South qilian accretionary belt (qilian orogen NW China). *J. Petrol* 60, 85–116. doi:10.1093/petrology/egy107

Yao, W. H., Li, Z. X., Li, W. X., Wang, X. C., Li, X. H., and Yang, J. H. (2012). Post-kinematic lithospheric delamination of the Wuyi–Yunkai orogen in South China: evidence from ca. 435Ma high-Mg basalts. *Lithos* 154, 115–129. doi:10.1016/j.lithos.2012.06.033

Yin, A., Manning, C. E., Lovera, O., Menold, C. A., Chen, X. H., and Gehrels, G. E. (2007). Early paleozoic tectonic and thermomechanical evolution of ultrahigh-pressure

(UHP) metamorphic rocks in the northern Tibetan plateau northwest China. *Int. Geol. Rev.* 49, 681–716. doi:10.2747/0020-6814.49.8.681

Yu, S. Y., Zhang, J. X., Li, H. K., Hou, K. J., Mattinson, C. G., and Gong, J. H. (2013). Geochemistry zircon U-Pb geochronology and Lu-Hf isotopic composition of eclogites and their host gneisses in the Dulan area North Qaidam UHP terrane: new evidence for deep continental subduction. *Gondwana Res.* 23, 901–919. doi:10.1016/j.gr.2012.07.018

Yuan, G. B., Wang, H. C., Li, H. M., Hao, G. J., Xin, T. H., Zhang, B. H., et al. (2002). Zircon U-Pb chronology and significance of gabbro in the Lvliangshan area. *Progress in Precambrian Res.* 01, 36-38+37-40. (in Chinese with English abstract).

Zhang, C., Roermund, H. V., Zhang, L. F., and Spiers, C. (2012). A polyphase metamorphic evolution for the Xitieshan paragneiss of the north Qaidam UHP metamorphic belt western China: in-situ EMP monazite- and U-Pb zircon SHRIMP dating. *Lithos* 136–139, 27–45. doi:10.1016/j.lithos.2011.07.024

Zhang, C., Zhang, L. F., Bader, T., Song, S. G., and Lou, Y. X. (2013). Geochemistry and trace element behaviors of eclogite during its exhumation in the Xitieshan terrane North Qaidam UHP belt NW China. *J. Asian Earth Sci.* 63, 81–97. doi:10.1016/j.jseaes.2012.09.021

Zhang, G. B., Ellis, D. J., Christy, A. G., Zhang, L. F., Niu, Y. L., and Song, S. G. (2009a). UHP metamorphic evolution of coesite-bearing eclogite from the Yuka terrane North Qaidam UHPM belt NW China. *Eur. J. Mineral.* 21, 1287–1300. doi:10.1127/0935-1221/2009/0021-1989

Zhang, G. B., Ireland, T., Zhang, L. F., Zhan, G., and Song, S. G. (2016). Zircon geochemistry of two contrasting types of eclogite: implications for the tectonic evolution of the North Qaidam UHPM belt northern Tibet. *Gondwana Res.* 35, 27–39. doi:10.1016/j.gr.2016.04.002

Zhang, G. B., Zhang, L. F., and Christy, A. G. (2013). From oceanic subduction to continental collision: an overview of HP–UHP metamorphic rocks in the North Qaidam UHP belt NW China. *J. Asian Earth Sci.* 63, 98–111. doi:10.1016/j.jseaes.2012.07.014

Zhang, G. B., Zhang, L. F., Song, S. G., and Niu, Y. L. (2009b). UHP metamorphic evolution and SHRIMP geochronology of a coesite-bearing meta-ophiolitic gabbro in the North Qaidam NW China. *J. Asian Earth Sci.* 35, 310–322. doi:10.1016/j.jseaes.2008.11.013

Zhang, J. X., Mattinson, C. G., Yu, S. Y., Li, J. P., and Meng, F. C. (2010). U-Pb zircon geochronology of coesite-bearing eclogites from the southern Dulan area of the North Qaidam UHP terrane northwestern China: spatially and temporally extensive UHP metamorphism during continental subduction. *J. Metamorph Geol.* 28, 955–978. doi:10.1111/j.1525-1314.2010.00901.x

Zhang, J. X., Yu, S. Y., and Mattinson, C. G. (2017). Early Paleozoic polyphase metamorphism in northern Tibet China. *Gondwana Res.* 41, 267–289. doi:10.1016/j.gr.2015.11.009

Zhang L., L., Chen, R. X., Zheng, Y. F., Li, W. C., Hu, Z. C., Yang, Y. H., et al. (2016). The tectonic transition from oceanic subduction to continental subduction: zirconological constraints from two types of eclogites in the North Qaidam orogen northern Tibet. *Lithos* 244, 122–139. doi:10.1016/j.lithos.2015.12.003

Zhang, Q., Ma, W. P., Jin, W. J., and Li, X. Y. (1995). Post orogenic gabbro in xin county henan: geochemical characteristics. *Geochemistry* 04, 341–350. (in Chinese with English abstract).

Zhang, X. H., Zhang, H. F., Tang, Y. J., Wilde, S. A., and Hu, Z. C. (2008). Geochemistry of permian bimodal volcanic rocks from central inner Mongolia north China: implication for tectonic setting and phanerozoic continental growth in central asian orogenic belt. *Chem. Geol.* 249, 262–281. doi:10.1016/j.chemgeo.2008.01.005

Zhang, Y. Q., Song, S. G., Yang, L. M., Su, L., Niu, Y. L., Allen, M. B., et al. (2017). Basalts and picrites from a plume-type ophiolite in the South qilian accretionary belt qilian orogen: accretion of a cambrian oceanic plateau? *Lithos* 278-281, 97–110. doi:10.1016/j.lithos.2017.01.027

Zhao, Z. X., Wei, J. H., Fu, L. B., Liang, S. N., and Zhao, S. Q. (2017). The Early Paleozoic Xitieshan syn-collisional granite in the North Qaidam ultrahigh-pressure metamorphic belt NW China: petrogenesis and implications for continental crust growth. *Lithos* 278-281, 140–152. doi:10.1016/j.lithos.2017.01.019

Zhu, X. H. (2011). *Geochemical and zircon U-Pb dating studies of the volcanics of Tanjianshan Group in the North Qaidam*. Dissertation. Northwest University (in Chinese with English abstract)

Zhu, T., Dong, Y. P., Wang, W., Xu, J. G., Ma, H. Y., and Charles, C. (2008). The geochemical characteristics and tectonic setting of volcanic rocks in Caotangou Group. *Northwest. Geol.* 01, 59–66. doi:10.3969/j.issn.1009-6248.2008.01.007

Zhu, X. H. (2021). *Magmatic response to early paleozoic tectonic transition in South qilian and North Qaidam and its constraints on orogenic process*. Dissertation: Northwest University. (in Chinese with English abstract).

Zhu, X. H., Chen, D. L., Liu, L., and Li, D. (2010). Zircon LA-ICP-MS U-Pb dating of the Wanggaxiu gabbro complex in the Dulan area, northern margin of Qaidam Basin, China and its geological significance. *Geol. Bull. China* 29, 227–236. (in Chinese with English abstract). doi:10.3969/j.issn.1671-2552.2010.02.006

Zhu, X. H., Chen, D. L., Liu, L., Wang, C., Yang, W. Q., Cao, Y. T., et al. (2012). Chronology and geochemistry of the mafic rocks in Xitieshan area, North Qaidam. *Geol Bull of China* 31 (12), 2079–2089. (in Chinese with English abstract).

Zhu, X. H., Chen, D. L., Liu, L., Zhao, J., and Zhang, L. (2014). Geochronology, heochemistry and significance of the Early Paleozoic back-arc basin type ophiolite in Lvliangshan area, North Qaidam. *Acta Petrol Sin.* 30, 822–834. (in Chinese with English abstract).